

# Rat retinal transcriptome

## Effects of aging and AMD-like retinopathy

Oyuna S. Kozhevnikova, Elena E. Korbolina, Nikita I. Ershov and Natalia G. Kolosova\*

Institute of Cytology and Genetics; Siberian Branch of the Russian Academy of Sciences (SB RAS); Novosibirsk, Russia

**Keywords:** aging, age-related macular degeneration, retinal transcriptome, RNA-Seq, OXYS rats

**Abbreviations:** AMD, age-related macular degeneration; RPE, retinal pigment epithelium; DE, differential expression; DEGs, differentially expressed genes; NGS, next generation sequencing; ECM, extracellular matrix; IFs, intracellular filaments; PCA, principal component analysis; FPKM, fragments per kilobase of exon model per million mapped fragments; GO, gene ontology; CNS, central nervous system

Pathogenesis of age-related macular degeneration (AMD), the leading cause of vision loss in the elderly, remains poorly understood due to the paucity of animal models that fully replicate the human disease. Recently, we showed that senescence-accelerated OXYS rats develop a retinopathy similar to human AMD. To identify alterations in response to normal aging and progression of AMD-like retinopathy, we compared gene expression profiles of retina from 3- and 18-mo-old OXYS and control Wistar rats by means of high-throughput RNA sequencing (RNA-Seq). We identified 160 and 146 age-regulated genes in Wistar and OXYS retinas, respectively. The majority of them are related to the immune system and extracellular matrix turnover. Only 24 age-regulated genes were common for the two strains, suggestive of different rates and mechanisms of aging. Over 600 genes showed significant differences in expression between the two strains. These genes are involved in disease-associated pathways such as immune response, inflammation, apoptosis, Ca<sup>2+</sup> homeostasis and oxidative stress. The altered expression for selected genes was confirmed by qRT-PCR analysis. To our knowledge, this study represents the first analysis of retinal transcriptome from young and old rats with biologic replicates generated by RNA-Seq technology. We can conclude that the development of AMD-like retinopathy in OXYS rats is associated with an imbalance in immune and inflammatory responses. Aging alters the expression profile of numerous genes in the retina, and the genetic background of OXYS rats has a profound impact on the development of AMD-like retinopathy.

### Introduction

Age-related macular degeneration (AMD) is the most common cause of blindness in people older than 60. Various environmental, dietary and genetic factors influence AMD pathogenesis.<sup>1,2</sup> The prevalence of AMD increases dramatically with age, and the normal process of aging is a potential risk and causative factor for AMD. Typical aging-related alterations of choroid, retinal pigment epithelium (RPE) and Bruch's membrane underlie the AMD pathogenesis, but the mechanisms that trigger the transition from normal age-related changes to the disease are not known. The changes that are common to normal aging of the retina and its diseased state are not known either. Although the last decade has seen great progress in understanding the pathophysiology of AMD, the molecular pathways underlying the onset and progression of AMD have yet to be described. It is, however, clear that AMD is a typical age-related disease and is caused in part by aging.<sup>3–6</sup> Aging is a complex process driven by diverse molecular pathways and biochemical events.<sup>7–12</sup> Initially, cellular aging is associated with

cellular hyperfunctions, hyperproliferation and hypersecretion (SASP), and only later it leads to organ damage and malfunctions.<sup>9,13–18</sup> The gradual decline in cellular functions associated with aging is not caused by changes in the expression of a few individual genes, but rather by cumulative alterations in the activity of numerous genes in many tissues.<sup>19</sup> Identification of the molecular pathways that can serve as potential therapeutic targets can be facilitated by high-throughput systems biological analyses, particularly at the proteome and transcriptome levels. Transcriptome analysis is one of the approaches aimed at identifying the genetic determinants of a disease and investigating its pathogenesis. Recent studies have shown that RNA sequencing utilizing next generation sequencing (NGS) technology has many advantages in comparison to earlier technologies. First, it is highly reproducible and has a much greater dynamic range than the microarray analysis. Second, it can measure the level of any transcripts present in the library within the constraints of the depth of coverage, including unknown genes, low-copy transcripts, different splice variants and non-coding RNAs.<sup>20–26</sup> Currently NGS is recognized as the leading technology allowing

\*Correspondence to: Natalia G. Kolosova; Email: kolosova@bionet.nsc.ru  
Submitted: 03/01/13; Revised: 04/25/13; Accepted: 04/26/13  
<http://dx.doi.org/10.4161/cc.24825>

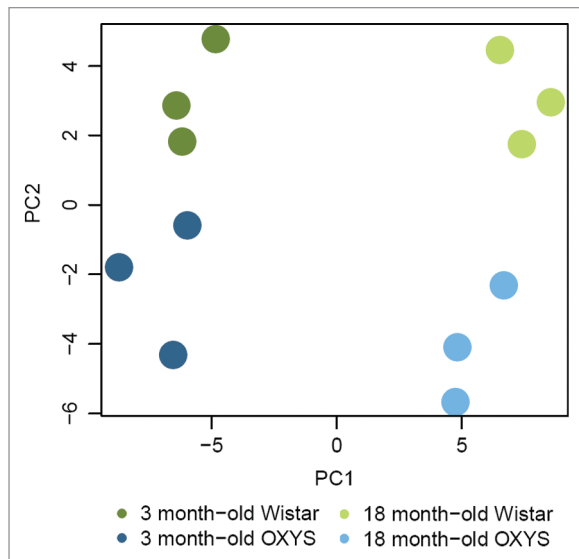


**Figure 1.** Principal component analysis (PCA) of RNA-Seq samples. PC1 and PC2 scores were visualized for a group of genes showing most variable differential expression with age. Different experimental groups tend to cluster together upon PCA, reflecting age (PC1), as well as strain (PC2) differences.

large-scale sequencing at low cost and driving molecular biology research forward.

AMD is complex and polygenic, resulting from cooperation of a variety of genes in the initiation and progression of the disease. Therefore, large-scale molecular biological experiments are needed in order to better understand the pathogenesis and progression of AMD and to identify new targets for AMD-directed therapeutics and diagnostics. The study of AMD is complicated by the limitations of animal models. We showed that senescence-accelerated OXYS rats are a suitable model for the study of pathogenesis and for investigation of possible therapeutic targets in AMD.<sup>27-34</sup>

OXYS rats spontaneously develop a phenotype similar to human geriatric disorders. In addition to retinopathy, this phenotype includes cataract, osteoporosis, high blood pressure and accelerated brain aging. These symptoms are strongly associated with aging, implying a common underlying process.

Manifestation of clinical signs of retinopathy in OXYS rats occurs by the age of about 3 mo against the background of a significantly reduced expression level of VEGF and PEDF genes due to the decline of the amount of retinal pigment epithelium cells and alterations in choroidal microcirculation. Significant pathological changes of RPE as well as clinical symptoms of advanced stages of retinopathy are observed in OXYS rats older than 12 mo and manifest themselves as excessive accumulation of lipofuscin in RPE regions adjacent to the rod cells, whirling extensions of the basement membrane into the cytoplasm. Eventually primary cellular degenerative changes develop in the RPE cells, lead to choriocapillaris atrophy and result in a complete loss of photoreceptor cells in the OXYS retina by the age of 24 mo.<sup>32</sup> Although QTLs on the first chromosome were detected, and the constructed congenic strains of animals display cataract and

retinopathy development,<sup>35</sup> the genetic basis of such accelerated senescent phenotype is still unknown.

To test the relationship between the development of retinopathy in OXYS rats with typical aging-related alterations of the transcriptome, we compared gene expression profiles in the retina of senescence-accelerated OXYS rats and control Wistar rats using high-throughput RNA sequencing (RNA-Seq). To our knowledge, this study represents the first analysis of retinal transcriptome in young and old rats with biologic replicates generated by RNA-Seq technology.

## Results

We compared gene expression profiles from retinas of 3- and 18-mo-old senescence-accelerated OXYS rats and age-matched control Wistar rats. In order to improve the quality and reliability of differential expression (DE) detection, we used three biological replicates. Analysis of RNA-Seq data presents major challenges in transcript assembly and abundance estimation because of the ambiguous assignment of reads to isoforms.<sup>36</sup> As many available software tools for DE analysis are becoming faster and easier to use, this makes it possible to use several different packages for DE testing in order to strengthen the list of DE candidates.<sup>37</sup> We used two different tools for differential expression analysis: Cufflinks pipeline<sup>36</sup> and DESeq<sup>38</sup> to assemble the transcripts. Gene abundances were quantified as fragments per kilobase of exon model per million mapped fragments (FPKM) for the Cufflinks method, and as the number of unique reads falling into the exons of the gene (read counts) for DESeq method. We identified about 15,300 transcripts expressed at least in three of the samples with FPKM greater than one. Differential expression analysis between the OXYS and Wistar strains as well as between the ages of 3 and 18 mo calculated by the two methods is summarized in Table S4.

The maximum of read counts was 15,7848 revealed by DESeq, and 12,046 (FPKM) by Cufflinks. The mean and median expression levels were 322 and 101 read counts calculated by DESeq and 43 and 10 FPKM normalized by Cufflinks, respectively, with FPKM value cutoff greater than one. The presence of these highly abundant as well as rare transcripts in the data set demonstrates that the library preparation and data analysis methods did not introduce any undesirable bias.<sup>23</sup> The most highly expressed transcripts common to OXYS and Wistar retinas were rod photoreceptor genes such as *Gnat1*, *Rho* and *Sag* (Table S2). This is consistent with the data from the mouse retina RNA-Seq by Gamsiz et al.<sup>21</sup>

Principle component analysis (PCA) in Wistar and OXYS samples was used to evaluate similarities or differences in gene expression patterns (Fig. 1). Four separate clusters of samples are seen at PC1-PC2 plot; each of them contains three biological replicates, indicating no potential sample mix-up. Data reveal that the age-affected genes show strain-dependent expression, suggesting that age-related gene expression changes in the retina may be unique to a single strain.

**Comparison of transcript differences revealed by two analyses.** We analyzed the sequence data using Cufflinks and DESeq

methods and found method-specific changes in transcript abundance. Using the stringent p value adjusted (FDR) filtering, Cufflinks detects more differentially expressed genes (DEGs) compared with DESeq. Most annotated DEGs were overlapped between methods. However, some transcripts were detected only by one of the methods. For example, crystallins and lens-specific genes were assigned as differentially expressed only by the Cufflinks method. A difference was also noted in the fold-changes for some genes uncovered by the two methods. The discrepancy between results can be attributed to differences in the alignment algorithms, filtering criteria and calculation of differential gene expression between the two methods. This discrepancy demonstrates that altered abundance of transcripts can be detected by combining two methods. This observation illustrates the importance of the choice of the method of analysis, which may affect the final results and conclusions from NGS data. For this reason, we thoroughly analyzed data generated by the two methods, considering their drawbacks, and created an integrated final list of DE genes. The final list of DE genes for all comparisons is shown in Table S5.

There are 496 genes that are differentially expressed in 3-month-old OXYS rats compared with age-matched Wistar rats; of these 390 are downregulated, and 106 are upregulated. When using a cutoff of > 2.0-fold, the numbers are 332 total, 286 downregulated and 46 upregulated. At 18 mo of age, there are 430 differentially expressed genes; of these 329 are downregulated, and 101 are upregulated in OXYS rats. With a cutoff of > 2.0-fold, the total number is 282 genes (229 downregulated and 53 upregulated). Approximately 40% of DEGs (190) are overlapping between the data sets corresponding to 3- and 18-month-old rats.

The total of 160 and 146 genes exhibited altered expression in the course of Wistar and OXYS aging, respectively, but only 24 genes are common. Among age-related DEGs 80 and 84 genes changed expression more than 2-fold in Wistar and OXYS rats, respectively.

Interestingly, among DE genes between strains, the majority of protein coding genes were downregulated in OXYS as shown by both methods. In addition, we should mention that a large percentage of DEGs has no annotated function, so they may represent new targets for future investigation in vision research.

The top genes with the highest fold expression differences between OXYS and Wistar retinas that are present both in the 3- and 18-month data sets, as well as age-related DEGs, are listed in Table 1. Notably, most of them have not been identified previously as associated with retinopathies. For example, among the most overexpressed genes in OXYS at both ages, we found a retrotransposed gene LOC100360791 of unknown function, a small proline-rich repeat protein 1A (Sprr1a) that has been proposed as a regeneration-associated marker in CNS,<sup>39,40</sup> and the key immunomodulatory peptide gene Slurp1 that is downregulated in proinflammatory conditions and participates in signal transduction, immune cell activation and cellular adhesion.<sup>41,42</sup> The most significantly overexpressed gene in the OXYS retina

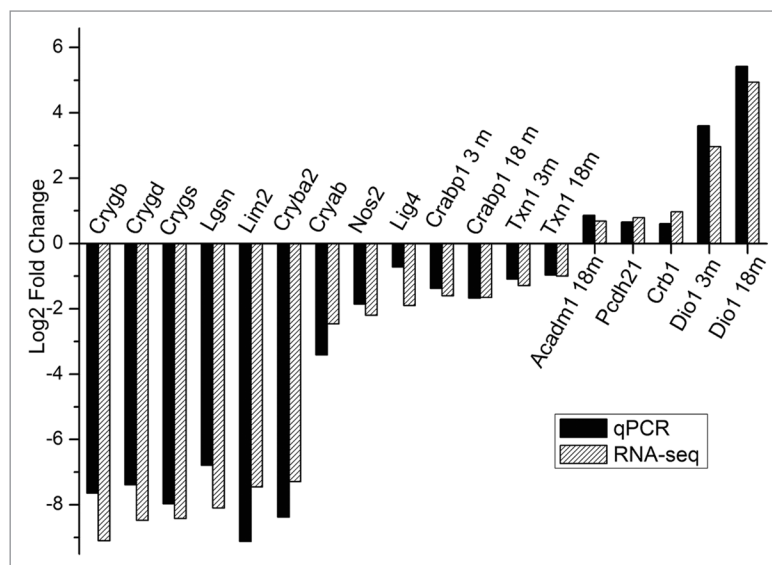


**Figure 2.** qRT-PCR validation of RNA-Seq results. Comparison of fold change (log<sub>2</sub> scale) in differential expression values determined by RNA-Seq (white) and qPCR (black) for DEGs.

is Dio1 (deiodinase, iodothyronine, type I, Fold Change > 31 at age of 18 mo), which regulates the balance of circulating thyroid hormone levels in tissues converting T<sub>4</sub> to T<sub>3</sub> by deiodination.<sup>43</sup>

**Confirmation of sequencing data by qRT-PCR.** To validate the RNA-Seq data, we performed quantitative RT-PCR. Fifteen DEGs were chosen based on RNA-Seq data, including seven genes encoding structural components of lens and crystallins, which were identified as strongly underexpressed by Cufflinks. RT-PCR confirmed that the chosen genes were significantly down/upregulated in the OXYS strain. The fold changes of OXYS vs. Wistar gene expression levels were consistent between RNA-Seq and RT-PCR data (Fig. 2). Only one gene, Lig4, showed a much lower fold change using RT-PCR than predicted from RNA-Seq data. Independent age-matched groups of animals were used for qPCR validation; therefore, our RNA-Seq results must be reliable.

**Pathway analysis.** To identify pathways and biological functions associated with DE genes than expected by chance, we used DAVID<sup>44</sup> and WebGestalt, (<http://bioinfo.vanderbilt.edu/webgestalt/option.php>). Pathway analysis was done for entire lists of DE genes (Table S6) and for separate up and downregulated groups (Table S7). The most representative gene ontology (GO) terms are shown in Figure 3. Alternative results of WebGestalt annotation for entire lists of DEGs are shown in Table S8.

**Age-associated transcriptome profiles.** The experimental design allowed us to identify pathways and biological functions associated with changes in the retinal transcriptome during aging in senescent-accelerated OXYS rats as well as in control Wistar rats, who have no signs of retinopathy. In both strains, the genes significantly downregulated with aging were associated with extracellular matrix organization (in Wistar: Lama1, Col3a1, Col1a2, Igf1, Postn, Sparc, Col1a1 and Col4a5; in OXYS: Aspn, Gpc3, Lum, Col3a1, Tgfb1, Eln, Col1a2, Col6a1, Col12a1, Col1a1, Col5a1 and Thbs4). We found that Wistar DE genes

**Table 1.** Differentially expressed genes (DEGs) with a fold change (FC) cutoff > 2.0 and adjusted p values < 0.05

Gene title	Gene Symbol	Gene ontology term	FC	p value
<b>A. Strain-related DEGs between Wistar and OXYS retinas common for 3- and 18-mo-old comparisons</b>				
Unknown; RGD: tumor protein, translationally-controlled 1	LOC100360791	unknown	-281,48	2.09E-04
WD repeat domain 63	Wdr63	unknown	-26,75	0,000244
Membrane-spanning 4-domains, subfamily A, member 8A	Ms4a8a	integral to membrane	-7,15	0,005734
Ly6-C antigen	Ly6c	CD59 antigen, Ly-6 antigen/uPA receptor-like	-6,28	8.84E-08
Tuftelin 1	Tuft1	biomineral formation	-5,84	2.52E-14
Ligase IV, DNA, ATP-dependent	Lig4	DNA repair, T cell differentiation, regulation of neuron apoptosis	-5,61	1.12E-10
Family with sequence similarity 3, member B	Fam3b	generation of a signal involved in cell-cell signaling, hormone transport	-5,12	3,98E-05
Glycoprotein hormone $\alpha$ 2	Gpha2	hormone activity	-4,63	0,000304
Similar to secreted Ly6/upar related protein 2	RGD1308195	unknown	-4,37	3,68E-05
NAD(P)H dehydrogenase, quinone 1	Nqo1	response to oxidative stress, regulation of apoptosis	-4,36	3,17E-08
Cystatin A (stefin A)	Csta	regulation of peptidase activity	-4,31	7,97E-05
Similar to hypothetical protein FLJ32859; uroplakin 1B	Upk1b	epithelial cell differentiation	-4,18	4.21E-12
Secretory leukocyte peptidase inhibitor	Slpi	enzyme inhibitor activity	-4,17	9.09E-04
Secreted Ly6/Plaur domain containing 1	Slurp1	biological adhesion, cytokine activity	-3,90	1.58E-10
Serine (or cysteine) peptidase inhibitor, clade B, member 5	Serp1n5	endopeptidase inhibitor activity, extracellular matrix organization	-3,74	2.48E-08
Family with sequence similarity 65, member C	Fam65c	unknown	-3,70	7,03E-13
Carboxylesterase 2 (intestine, liver)	Ces2c	lipid metabolism	-3,43	0,003429
Tissue factor pathway inhibitor 2	Tfpi2	blood coagulation	-3,38	0,00111
Similar to phosducin-like	LOC690155	unknown	-3,34	0,010746
G protein-coupled receptor 115	Gpr115	G-protein coupled receptor protein signaling pathway, neuropeptide signaling pathway	-3,29	0,031864
Aldehyde dehydrogenase 3 family, member A1	Aldh3a1	response to hypoxia, regulation of cell proliferation	-3,36	2.47E-03
Interferon induced transmembrane protein 1	Ifitm1	signal transduction, regulation of cell proliferation	-3,18	2,67E-07
Small proline-rich protein 1A-like	Sprr1a	peptide cross-linking	-3,23	9,39E-07
Interleukin 18	Il18	angiogenesis, response to hypoxia, immune response	-3,15	0,002015
Similar to keratin 6 $\alpha$	RGD1562494	unknown	-3,16	5,06E-08
Similar to hypothetical protein FLJ20171	Esrp1	regulation of RNA splicing	-3,12	0,031256
Similar to 2210023G05Rik protein	Ces2g	unknown	-3,09	0,001939
Glutathione peroxidase 2	Gpx2	regulation of inflammatory response	-3,09	0,003187
Annexin A8	Anxa8	calcium ion binding	-3,07	3,06E-08
ENSRNOG00000020628	Unknown	unknown	-3,07	0,000403
Fibroblast growth factor binding protein 1	Fgfbp1	cell-cell signaling	-3,05	0,044562
Inositol (myo)-1(or 4)-monophosphatase 2	Impa2	phosphate metabolic process, metal ion binding	-3,03	4,93E-05

(A) Strain-related DEGs common for 3- and 18-mo-old comparisons between Wistar and OXYS retinas. Specified values of fold change and adjusted p values refer to the 18 mo age. (B) Age-related DEGs in retina of 18 mo Wistar compared with 3-mo-old Wistar (FC cutoff > 2.0 and adjusted p values < 0.05). (C) Age-related DEGs in retina of 18 mo OXYS compared with 3-mo-old OXYS rats (FC cutoff > 2.0 and adjusted p values < 0.05). The full results in **Table S2**.

**Table 1.** Differentially expressed genes (DEGs) with a fold change (FC) cutoff > 2.0 and adjusted p values < 0.05 (continued)

Gene title	Gene Symbol	Gene ontology term	FC	p value
RAB25, member RAS oncogene family	Rab25	regulation of transcription, intracellular signaling cascade	-3,02	0,005032
Similar to normal mucosa of esophagus specific 1-like	LOC100364608	unknown	-2,96	0,035903
Aquaporin 3	Aqp3	water transport, immune system process	-2,91	2,61E-07
Prostate stem cell antigen	Psca	Ly-6 antigen / uPA receptor-like	-2,89	1,2E-07
Calmodulin 4	Calm4	calcium ion binding	-2,89	6.24E-07
Zinc finger protein 185; similar to zinc finger protein 185	Zfp185	cell junction	-2,88	0,027731
Ly6/Plaur domain containing 3	Lypd3	cell-matrix adhesion	-2,88	7,8E-06
Tumor-associated calcium signal transducer 2	Tacstd2	signal transduction, visual perception	-2,87	2,28E-06
Cytochrome P450, family 3, subfamily a, polypeptide 9	Cyp3a9	electron carrier activity, drug catabolic process	-2,85	0,000556
Cellular retinoic acid binding protein 1	Crabp1	vitamin binding	-3,14	7.95E-13
Sciellin	Scel	epidermis development	-2,70	0,002748
Syndecan 1	Sdc1	inflammatory response, response to oxidative stress, Wnt receptor signaling pathway	-2,83	1,21E-07
WDNM1 homolog	LOC360228	response to cytokine stimulus, fat cell differentiation	-2,81	0,017522
PERP, TP53 apoptosis effector	Perp	apoptosis, regulation of cell death	-2,76	2,94E-07
Similar to RIKEN cdna 1810065E05	Pinlyp	phospholipase inhibitor activity	-2,71	0,002742
EPS8-like 1	Eps8l1	intracellular signaling cascade	-2,70	0,014653
Histocompatibility 2, T region locus 23;	Rt1-S3	immune response	-2,69	4,93E-05
Kruppel-like factor 5	Klf5	angiogenesis, regulation of transcription	-2,68	0,006303
Radical S-adenosyl methionine domain containing 2	Rsad2	immune response	-2,67	2.51E-02
Similar to hypothetical protein FLJ22671	RGD1563692	unknown	-2,67	0,000113
Epithelial membrane protein 1	Emp1	cell growth	-2,65	0,001939
Similar to specifically androgen-regulated protein	LOC498222	unknown	-2,62	0,01258
Prostaglandin reductase 1	Ptgr1	response to toxin, alcohol dehydrogenase (NAD) activity	-2,62	1,12E-07
Capping protein (actin filament), gelsolin-like	Capg	regulation of actin cytoskeleton organization	-2,56	2,15E-05
Similar to uroplakin 3B isoform b	Upk3bl	unknown	-2,54	1,49E-05
EPS8-like 2	Eps8l2	intracellular signaling cascade	-2,53	3E-06
PDZ and LIM domain 2	Pdlim2	focal adhesion	-2,49	0,004421
S100 calcium binding protein A11 (caliz-zarin)	S100a11	S100 protein binding, calcium ion binding	-2,47	2,96E-05
UDP-N-acetyl- $\alpha$ -D-galactosamine:polypeptide N-acetylgalactosaminyltransferase 12 (galnac-T12)	Galnt12	protein glycosylation	-2,46	0,039745
Nitric oxide synthase 2, inducible	Nos2	response to hypoxia, regulation of blood pressure, signal transduction	-2,44	0,037486
Tripartite motif-containing 16	Trim16	regulation of transcription, DNA-dependent, positive regulation of signal transduction	-2,44	0,019678
Epithelial cell adhesion molecule	Epcam	positive regulation of cell proliferation	-2,40	0,010797

(A) Strain-related DEGs common for 3- and 18-mo-old comparisons between Wistar and OXYS retinas. Specified values of fold change and adjusted p values refer to the 18 mo age. (B) Age-related DEGs in retina of 18 mo Wistar compared with 3-mo-old Wistar (FC cutoff > 2.0 and adjusted p values < 0.05). (C) Age-related DEGs in retina of 18 mo OXYS compared with 3-mo-old OXYS rats (FC cutoff > 2.0 and adjusted p values < 0.05). The full results in **Table S2**.

**Table 1.** Differentially expressed genes (DEGs) with a fold change (FC) cutoff > 2.0 and adjusted p values < 0.05 (continued)

Gene title	Gene Symbol	Gene ontology term	FC	p value
Annexin A2	Anxa2	angiogenesis, vasculature development, extracellular organization	-2,31	0,000665
Lymphocyte antigen 6 complex, locus G6E	Ly6g6e	leukocyte antigen, signal transduction	-2,25	0,006756
Lectin, galactoside-binding, soluble, 3	Lgals3	extracellular matrix organization	-2,24	0,000237
Mal, T-cell differentiation protein 2	Mal2	lipid raft	-2,05	0,000805
Placenta-specific 8	Plac8	regulation of transcription, negative regulation of apoptotic process	-2,09	0,016989
Glycolipid transfer protein	Gltp	lipid transport, lipid localization	-2,03	0,001796
Thioredoxin 1	Txn1	regulation of transcription, oxidative stress, electron transport chain	-2,03	0,001001
Zinc finger protein 691	Znf691	DNA binding	2,14	0,030785
Beta-1,4-N-acetyl-galactosaminyl transferase 3	B4galnt3	acetylgalactosaminyltransferase activity	2,19	0,006226
Mediator complex subunit 20	Med20	regulation of RNA metabolic process	2,40	9,03E-08
Calcium/calmodulin-dependent protein kinase 1G	Camk1g	intracellular signaling cascade, calcium-mediated signaling	2,47	0,00018
Laminin, $\beta$ 3	Lamb3	cell adhesion	2,59	1.89E-05
Unknown	LOC690806	unknown	2,67	0,02043
Kinesin family member 2C	Kif2c	microtubule cytoskeleton organization, cell cycle	2,87	0,011592
Inducible carbonyl reductase-like	LOC100360507	unknown	3,16	0,008711
Serine hydrolase-like 2	Serhl2	hydrolase activity, provisional	3,22	0,001306
Similar to RIKEN cDNA 2210421G13	LOC100365656	unknown	3,38	0,03259
ENSRNOG00000004090	Unknown	unknown	8,44	4,44E-09
Similar to Hmgb1 protein	Hmg11	eye development, regulation of RNA, DNA metabolic process	13,78	1,11E-07
Transmembrane protein 14C	LOC100361993	heme biosynthetic process	20,12	5,55E-08
Otopetrin 3	Otop3	zinc ion binding	22,04	5.54E-25
Deiodinase, iodothyronine, type I	Dio1	generation of precursor metabolites and energy, hormone metabolic process	30,87	1.98E-66
Testis specific 10 interacting protein	Tsga10ip	unknown	35,16	0,003718
Similar to S100 calcium-binding protein, ventral prostate	RGD1562234	unknown	up	4,11E-28
UDP glucuronosyltransferase 2 family, polypeptide B17	Ugt2b1	drug metabolic process	up	0,009212
<b>B. Age-related DEGs between 3 mo and 18 mo Wistar retinas</b>				
Interferon-induced protein with tetratricopeptide repeats 1	Dio1	cytokine-mediated signaling pathway	15,79	0,020378
N-acetylglutamate synthase	Tsga10ip	glutamate metabolic process	12,39	0,021974
Predicted gene 239	RGD1562234	regulation of transcription	3,52	0,00011
Coiled-coil domain containing 125	Ugt2b1	intermediate filament cytoskeleton	3,06	0,036548
Adiponectin, C1Q and collagen domain containing	Dio1	response to hypoxia, regulation of blood pressure, regulation of apoptosis, regulation of I-kappaB kinase/NF-kappaB cascade	11,25	0,026368
Glucagon-like peptide 1 receptor	Tsga10ip	intracellular signaling cascade, regulation of neuron apoptosis, regulation of RNA metabolic process	5,68	0,036548

(A) Strain-related DEGs common for 3- and 18-mo-old comparisons between Wistar and OXYS retinas. Specified values of fold change and adjusted p values refer to the 18 mo age. (B) Age-related DEGs in retina of 18 mo Wistar compared with 3-mo-old Wistar (FC cutoff > 2.0 and adjusted p values < 0.05). (C) Age-related DEGs in retina of 18 mo OXYS compared with 3-mo-old OXYS rats (FC cutoff > 2.0 and adjusted p values < 0.05). The full results in **Table S2**.

**Table 1.** Differentially expressed genes (DEGs) with a fold change (FC) cutoff > 2.0 and adjusted p values < 0.05 (continued)

Gene title	Gene Symbol	Gene ontology term	FC	p value
Down syndrome critical region homolog 6 (human)	RGD1562234	negative regulation of transcription	4,04	0,037642
Leukocyte receptor tyrosine kinase	Ugt2b1	cell surface receptor linked signal transduction	3,31	0,008951
KISS1 receptor	Dio1	MAPKKK cascade, calcium-mediated signaling	3,19	0,044381
Recombination signal binding protein for immunoglobulin kappa J region-like	Tsga10ip	regulation of transcription	3,17	9,76E-06
SEC14-like 3 (S. Cerevisiae)	RGD1562234	lipid binding	3,15	0,002527
Beta-1,4-N-acetyl-galactosaminyl transferase 3	Ugt2b1	acetylgalactosaminyltransferase activity	3,12	0,002258
Piwi-like 2 (Drosophila)	Dio1	RNA processing, regulation of translation	2,99	1,46E-07
Interleukin 18	Tsga10ip	angiogenesis, response to hypoxia, immune response	2,98	0,019713
Troponin T type 2 (cardiac)	RGD1562234	muscle tissue development	2,97	0,036985
Alcohol dehydrogenase 7 (class IV), mu or sigma polypeptide	Adh7	hormone metabolic process, alcohol catabolic process	2,85	1,35E-06
Cadherin 19, type 2	Cdh19	cell adhesion	2,52	0,007255
Prodynorphin	Pdyn	regulation of synaptic transmission	2,50	0,00325
Chloride intracellular channel 3	Clic3	ion transport	2,33	0,037407
Laminin, $\beta$ 3	Lamb3	cell adhesion	2,28	0,009289
Ankyrin repeat and BTB (POZ) domain containing 2	Abtb2	regulation of cell growth	2,25	0,000134
DENN/MADD domain containing 2C	Dennd2c	guanyl-nucleotide exchange factor activity	2,13	0,046743
Similar to Enolase	F1ltp6_rat	unknown	-9,59	0,021974
S100 calcium binding protein A9	S100a9	leukocyte migration, inflammatory response	-9,43	0,04917
Myxovirus (influenza virus) resistance 2	Mx2	response to virus	-4,96	4,69E-06
Similar to guanylate binding protein family, member 6	LOC685067	immune response	-4,73	4,53E-05
Guanylate binding protein 5	Gbp5	immune response	-2,89	0,003652
Calcitonin-related polypeptide, $\beta$	Calcb	G-protein coupled receptor protein signaling pathway, regulation of blood vessel size	-4,71	0,036985
Chemokine (C-X-C motif) ligand 2	Cxcl2	inflammatory response, immune response	-4,42	0,031517
Collagen, type III, $\alpha$ 1	Col3a1	vasculature development, regulation of immune process, extracellular matrix organization, axon guidance	-3,69	1,46E-07
Bifunctional methylenetetrahydrofolate dehydrogenase/cyclohydrolase, mitochondrial	Mthfd2	coenzyme metabolic process	-3,51	4,84E-07
Collagen, type I, $\alpha$ 1	Col1a1	vasculature development, response to oxidative stress	-3,10	1,38E-09
Collagen, type I, $\alpha$ 2	Col1a2	vasculature development, signal transduction, regulation of blood pressure	-3,07	2,88E-10
Deiodinase, iodothyronine, type I	Dio1	generation of precursor metabolites and energy, hormone metabolic process	-2,99	0,003916
Growth differentiation factor 15	Gdf15	cell-cell signaling, cytokine activity	-2,92	0,000483
Solute carrier family 26, member 3	Slc26a3	ion transport	-2,26	0,019659
Insulin-like growth factor 2 binding protein 2	Igf2bp2	regulation of translation, regulation of cytokine production	-2,08	0,01264
<b>C. Age-related DEGs between 3 mo and 18 mo OXYS retinas</b>				
Endothelin 2	Edn2	regulation of immune system process, calcium-mediated signaling	10,39	0,00175

(A) Strain-related DEGs common for 3- and 18-mo-old comparisons between Wistar and OXYS retinas. Specified values of fold change and adjusted p values refer to the 18 mo age. (B) Age-related DEGs in retina of 18 mo Wistar compared with 3-mo-old Wistar (FC cutoff > 2.0 and adjusted p values < 0.05). (C) Age-related DEGs in retina of 18 mo OXYS compared with 3-mo-old OXYS rats (FC cutoff > 2.0 and adjusted p values < 0.05). The full results in **Table S2**.

**Table 1.** Differentially expressed genes (DEGs) with a fold change (FC) cutoff > 2.0 and adjusted p values < 0.05 (continued)

Gene title	Gene Symbol	Gene ontology term	FC	p value
Lipocalin 2	Lcn2	transport, response to biotic stimulus	5,04	0,000108
Ladinin 1	Lad1	structural molecule activity	3,99	1,32E-07
Protein Kinase C, Gamma	Prkcg	protein modification process, signal transduction	3,95	1,9E-12
Secreted Ly6/Plaur Domain Containing 1	Slurp1	biological adhesion, cytokine activity	3,74	0,012244
Similar To Chromosome 11 Open Reading Frame 9	Rgd1562127	regulation of gene expression	3,31	0,000482
RT1 class Ia, Locus A2	Rt1-a2	immune response, regulation of response to stress	3,07	1,39E-07
Piwi-Like 2 (Drosophila)	Piwil2	RNA processing, regulation of translation, cell cycle	2,38	0,000748
Ankyrin Repeat And BTB (POZ) Domain Containing 2	Abtb2	regulation of cell growth	2,24	0,00026
Zinc Finger CCCH Type, Antiviral 1	Zc3hav1	regulation of immune response, response to stress	2,18	0,010647
7sk	7sk	unknown	-6,58	0,0005
Fatty Acid Binding Protein 4, Adipocyte	Fabp4	cytokine production, regulation of gene expression, inflammatory response	-5,61	0,006814
Collagen, Type III, Alpha 1	Col3a1	vasculature development, regulation of immune system process, extracellular matrix organization	-5,47	1,99E-13
Collagen, Type I, Alpha 2	Col1a2	vasculature development, signal transduction, regulation of blood pressure	-4,80	2,0E-10
Collagen, Type I, Alpha 1	Col1a1	vasculature development, response to oxidative stress	-4,63	4,08E-10
Lumican	Lum	extracellular matrix organization, neurological system process, sensory perception of light stimulus	-4,24	5,11E-06
Extracellular Matrix Protein 2	Ecm2	extracellular matrix organization	-3,57	0,006041
Insulin-Like Growth Factor 2 Mrna Binding Protein 2	Igf2bp2	regulation of gene expression, regulation of cytokine production	-2,77	4,62E-06
E9psm5_Rat	E9PSM5_RAT	unknown	-2,69	0,004592
F1m7f8_Rat	F1M7F8_RAT	unknown	-2,60	0,005421
ENSRNOG00000043936	Unknown	unknown	-2,15	0,02222

(A) Strain-related DEGs common for 3- and 18-mo-old comparisons between Wistar and OXYS retinas. Specified values of fold change and adjusted p values refer to the 18 mo age. (B) Age-related DEGs in retina of 18 mo Wistar compared with 3-mo-old Wistar (FC cutoff > 2.0 and adjusted p values < 0.05). (C) Age-related DEGs in retina of 18 mo OXYS compared with 3-mo-old OXYS rats (FC cutoff > 2.0 and adjusted p values < 0.05). The full results in **Table S2**.

downregulated with aging, included genes involved in immune response (Gbp5, Loc685067, Msh3, Cxcl3, Cxcl2, Oas1b, Cxcl6 and Gbp2), response to nutrient levels (Acadm, Igf1, Asns, Sparc, Col1a1 and Psph), aminoacyl-tRNA biosynthesis (Iars, Tars, Cars, Aars, Mars and RGD1305089) and cytokine activity (Cxcl3, Cxcl2, Cxcl6 and Gdf15). Furthermore, genes participating in the negative regulation of transcription (Rarg, Nab2, Pparg, Per2, Fabp4 and Hsf4), blood circulation and regulation of blood pressure (Hrh3, Pparg, Myh6, Adipoq and Glp1r) were significantly upregulated in the retina of old Wistar rats compared with young rats. Also, 18-mo-old Wistar rats showed a higher expression level of immune response genes (Il20rb, C4b, C6, Il1rl2, Il18 and Cfd) and genes involved in regulation of synaptic transmission (Kiss1r, Grm2, Bcan and Pdyn) compared with 3-mo-old rats. In the course of aging of the OXYS retina, we observed significant downregulation of genes associated with blood vessel development and cell adhesion (Col3a1, Eln, Col1a2, Col1a1, Col5a1 and Thbs4) and sensory perception of light stimulus (Pde6c, Opn1mw, Col1a1, Pde6h and Aanat). For

example, the expression of subunits (Pde6h and Pde6c) of retinal cone cGMP-phosphodiesterase, a key enzyme in visual transduction, was decreased, pointing indirectly to disturbances of photoreceptor integrity and function. Interestingly, the aging OXYS retina also shows upregulated genes associated with MHC class I protein complex (Rt1-A2, Rt1-M5, Rt1-Ce5 and Rt1-T24-1), blood vessel morphogenesis (Il18, Ntrk2, Zc3h12a and Fgf2) and protein kinase activity (Map3k5, EphA6, Rps6ka2, Mapk4, Ntrk2, Prkcg and Alk). Full results with p values are available in **Table S4**.

**Downregulated pathways in OXYS at age 3 mo.** We found that downregulated DE genes at 3 mo are enriched in genes generally associated with immune response (34) and response to stress (25). In particular, this group includes inflammatory response, response to oxidative stress (10), stress-activated protein kinase signaling pathway (Wnt7b, Tnf, Myd88, Rgd1306565 and Cryab), cytokine activity (10), MHC class I protein complex (Rt1-M3-1, Rt1-Ce5, Rt1-S3 and Rt1-N3). We also found the enrichment for the GO terms intermediate filament cytoskeleton



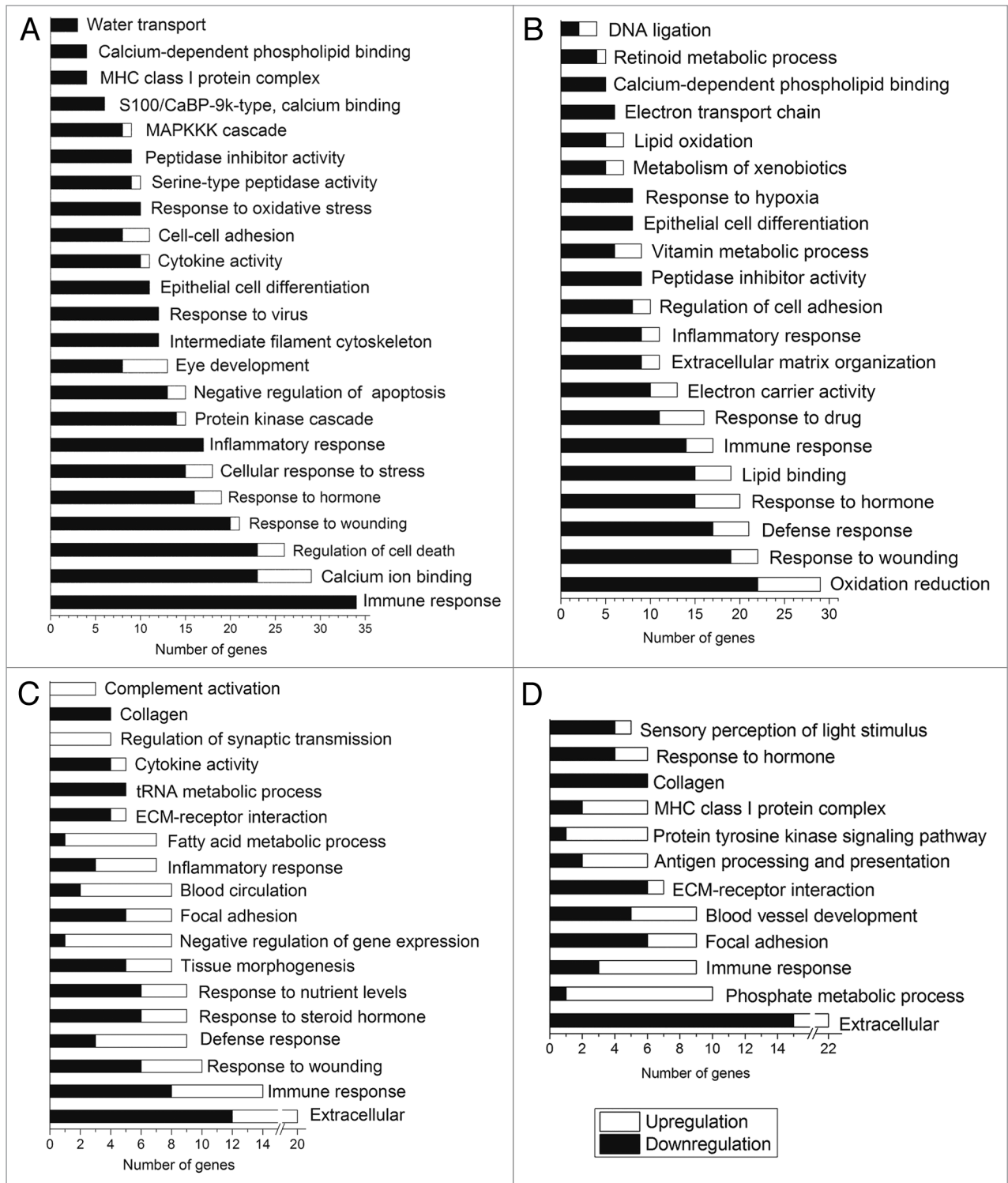


**Figure 3.** The most representative enriched gene ontology categories for differentially expressed genes in retinas: (A) between 3-mo-old OXYS and Wistar rats; (B) between 18-mo-old OXYS and Wistar rats; (C) between 3-mo and 18-mo-old Wistar rats; (D) between 3-mo and 18-mo-old OXYS rats.

(12), GTPase activity (7), negative regulation of apoptosis (13), calcium ion binding (23), serine-type peptidase activity (9) and others (Table S6).

**Upregulated pathways in OXYS rats at age 3 mo.** We found that the genes upregulated in OXYS retina at the age of 3 mo

are unexpectedly associated with phototransduction (Opn1mw, Opn1sw and Gnat2), eye development (Rax, Crb1, Hmg11, Rbp3 and Gnat2) and nuclear lumen (10) (Table S6). For the KEGG pathways analysis, we found 3 genes involved in Inositol phosphate metabolism (Miox, Plcd3, Itpka).

**Downregulated pathways in OXYS rats at age 18 mo.** We found that the downregulated DE genes at the age of 18 mo are enriched in response to wounding (19), oxidation-reduction (22), extracellular structure organization (9), immune response (14), inflammatory response (9), response to hypoxia (8), regulation of cell adhesion (8), fatty acid oxidation (Cd36, Adh7, Decr1, Adipoq and Alox12), electron transport chain (Nd4l, Cox8b, Txn1, Ndufa10, Glrx1 and Etf) and antigen processing and presentation (Rt1-A2, Rt1-Ce7, Rt1-S3 and Tapbp). For INTERPRO categories, we found enrichment in annexin (Anxa7, Anxa8, Anxa4 and Anxa2) and thioredoxin fold (Gpx2, Gstm4, Pdilt, Txn1, Clic1, Slc39a4 and Glrx1). For the KEGG pathways analysis, we found downregulated genes involved in the metabolism of xenobiotics by cytochrome P450 (Gstm4, Cyp1a1, Adh7, Cyp3a9 and Aldh3a1) (Table S6).

**Upregulated pathways in OXYS rats at age 18 mo.** OXYS DEGs upregulated at 18 mo included genes that participate in the regulation of hormone levels (Rdh8, Cyp11b1, Cyp11b2, Dio1 and Vgf), negative regulation of nucleobase metabolic process (Ciita, Gtpbp4, Hmgb2, Msh3, Hmg11l, Drd4 and Pax4), oxidation reduction (7), DNA ligation (Hmgb2 and Hmg11l) and neuron projection (7).

## Discussion

Our study represents the first analysis of retinal transcriptome in young and old rats with biologic replicates generated by RNA-Seq technology. As expected, we observed transcriptional alterations in a variety of genes in the retina due to the genetic background and aging process.

Pro-inflammation is one of hallmarks of aging.<sup>45-47</sup> The inflammatory responses observed in AMD patients and animal models are similar to those observed in normal aging eyes (with greater severity in AMD), suggesting that the causative factors for AMD are probably the same as those that exist in the normal aging retina, but these factors act with greater magnitude.<sup>48-50</sup> Our comparison of transcriptome profiles of aging Wistar and OXYS retinas showed several altered pathways in common, such as immune response and extracellular organization, but these common pathways consist of different genes in the two strains of rats. We found only 24 genes whose expression level changes with aging in both Wistar and OXYS rats, suggesting that the rates and mechanisms of age-related alterations in the retina are different between the two strains. Age-related differences were found in the expression of numerous genes participating in the modulation of the immune response and downregulation of collagens. A core set of extracellular matrix genes were dysregulated both during normal aging and in AMD-like retinopathy. The present results are in good agreement with previous studies. The inflammatory response and cytokine activity gene sets show an increasing trend in expression with age in different tissues and species, suggesting that inflammation becomes more active with age.<sup>19,48,49,51,52</sup>

At both ages in OXYS retinas, genes that were underexpressed compared with Wistar rats included many regulators of immunity, such as leukocyte markers (e.g., Cd24 and Tlr2),

chemokines (e.g., Cxcl2, Cxcl3 and Ccl6), cytokines (e.g., Il1a and Il18), complement components (C6 and Cfd), interferon-inducible proteins (e.g., Irf1, Isg20 and Ifi47) and MHC (major histocompatibility complex) genes (e.g., Rt1-A1 and Rt1-Ce7). For instance, a dramatic decrease in Nlrp6 expression (FC = -38) was seen in the comparison at age 18 mo. It is noteworthy that recently Nlrp6 has been shown to negatively regulate inflammatory signaling and host defense.<sup>53</sup> Such alterations can lead to abnormal or inadequate immune activity.

There is a growing body of evidence of an important role of immunological (including inflammatory) events in AMD pathogenesis.<sup>54,55</sup> Genome-wide association study studies have revealed several loci encoding proteins of the immune-related pathways that have a strong association with AMD-Cfh, Fb/C2, C3, C5, human leukocyte antigen (HLA) locus, Cx3cr1, Ccr3, Tlr3 and Tlr4.<sup>56-58</sup> Components of drusen and the retinal lesions in advanced AMD can initiate and promote inflammatory response, as well as innate adaptive immune reactions, such as a release of cytokines/chemokines, macrophage recruitment, microglia accumulation in subretinal space, complement activation and inflammatory oxidative stress.<sup>57</sup> Similar inflammatory mechanisms have been reported in other degenerative diseases characterized by accumulation of debris that can no longer be eliminated via the usual routes, such extracellular plaques in Alzheimer disease and deposits in atherosclerosis.<sup>47,59-63</sup> It is postulated that accumulation of drusen triggers local inflammation that can provoke a systemic immune response.<sup>64,65</sup> But the situation is more complicated, because cell-based inflammatory responses within the RPE/choroid were detectable at the earliest potential stage of the disease prior to vision loss and drusen accumulation.<sup>1</sup> This means inflammation and activation of the complement cascade are involved in the formation of drusen, a hallmark of AMD.<sup>55,60</sup>

We observed a downregulated profile of immune system genes that differs from previously described murine AMD model.<sup>24</sup> Recently Newman et al.<sup>1</sup> identified over 50 annotated genes enriched in cell-mediated immune responses that are globally overexpressed in RPE-choroid AMD phenotypes. In particular, they found upregulation of both complement and major histocompatibility complex I genes. But gene knockouts of some immune effectors can also lead to retina abnormalities. Remarkably, murine models with targeted inflammatory genes relevant to AMD, such as Cfh<sup>-/-</sup>, Ccl2<sup>-/-</sup>, Ccr2<sup>-/-</sup>, Cx3cr1<sup>-/-</sup> and Ccl2<sup>-/-</sup>/Cx3cr1<sup>-/-</sup> have many features of AMD.<sup>66</sup> For example, aged mice deficient in chemokine (Ccl2<sup>-/-</sup>) and its corresponding receptor (Ccr2<sup>-/-</sup>), a model of impaired macrophage recruitment, develop drusen formation, RPE accumulation of lipofuscin and complement factors as well as choroidal neovascularization.<sup>67</sup> It is possible that at early stages, macrophages perform the beneficial, long-term housekeeping role of scavenging deposits such as drusen.<sup>68</sup> Ccl2<sup>-/-</sup> and Ccr2<sup>-/-</sup> murine models of AMD suggest a protective role of macrophages in AMD pathogenesis. This chemokine deficiency results in impaired accumulation of macrophages at sites of inflammation, which impedes macrophage-mediated clearance of drusen components, leading to the generation of deposits.<sup>67</sup> The observed downregulated profile of immune system genes in OXYS rat also can be explained by

insufficient accumulation of macrophages in the retina due to impaired adhesion and failure of macrophage extravasation into tissues.

There are several possible explanations of the downregulated immune-response profile of the retinal transcriptome of OXYS rats. Inflammatory response mediated by the complement system and cytokines is a potent mechanism of host defense against pathogens and diseased cells; therefore it must be tightly regulated.<sup>65</sup> We observed impairment of appropriate inflammatory response in OXYS rats in other OXYS tissues when modeling collagen-induced arthritis (Kolossova et al., in preparation). In addition, we previously found a reduced level of delayed hypersensitivity reaction and a decline of T cell-mediated immunity in OXYS rats.<sup>69</sup> One possible cause of the observed immune imbalance can be attributed to the accelerated thymus involution in OXYS rats.<sup>70</sup> Thymus involution is one of the most important constituents of a decline of the immune system with age.<sup>50</sup> Immune imbalance provoked by accelerated thymic involution can create a specific metabolic background for development and progression of retinopathy in OXYS rats as one of the many manifestations of the accelerated senescence. Apparently the observed transcriptome dynamics of the immune system-related genes are associated with immunosenescence, a progressive and generalized deterioration of immune functions that affects all cells and organs of the innate and adaptive immune systems.<sup>70,72</sup> Also the altered cellular immune responses observed in OXYS retina may be the result of a dysregulation of inter- and intracellular signal transduction.

While the importance of immune response and complement system in AMD progression was well established in the past 10 years, so far it remains unclear whether and how other inflammation-mediated pathways, including the cytokine system, contribute to the development and progression of early AMD.<sup>73</sup> Unexpectedly, recent studies reveal that a number of immune molecules, such as cytokines, complement components and MHC proteins, in addition to their immunological roles, are essential for the establishment, function and modification of synaptic connections, activity-dependent refinement in the visual system and long-term and homeostatic plasticity.<sup>74,75</sup> Although it has long been assumed that complement activation augments immune responses, which in turn initiate AMD pathogenesis, evidence is emerging about a novel role of the complement in retinal degeneration. Yu et al.<sup>76</sup> have shown that C3aR- and C5aR-mediated signaling was necessary to maintain normal retinal function and structure unrelated to immune response. Therefore, we can cautiously assume that such a decrease of immune activity may be associated with systemic neurodegeneration processes in OXYS rats.

Many of the DEGs observed in the present study mediate stress and wound responses. RPE cells are important for the maintenance of the blood-retina barrier and retinal neurons and must participate in mechanisms protecting retina against oxidative stress generated by exposure to light and high oxygen tension.<sup>24</sup> With age, RPE becomes overwhelmed with cellular debris and vitamin A metabolites, such as A2-E (a toxic vitamin A dimer). When present in excessive levels, lipofuscin and A2-E damage

RPE, leading to the atrophy of photoreceptors and choriocapillaris.<sup>65</sup> Compared with Wistar rats, the OXYS strain displayed decreased expression of key gene families needed by RPE to cope with such stress. Among them are participants of the JNK cascade: stress-activated protein kinase signaling pathway (Tnf, Il1a, Wnt7b, Il1rn, Cbs, Myd88 and RGD1306565).

We discovered an abundance of  $\alpha$ ,  $\beta$  and  $\gamma$ -crystallin family transcripts in the retina samples. Large expression changes of mRNA levels of crystallins were observed between retinas of different rats according to the RNA-Seq data. Due to the high dispersion, DESeq did not consider them as DE. The variations in expression for all crystallins examined were evident in the qPCR confirmation analysis in the independent groups of animals. But in OXYS retinas, the mean levels of crystallin mRNA expression were always below Wistar levels. Significant individual variation in the expression level of some crystallins in the retina was shown earlier.<sup>77</sup> The high level of variability in crystallin transcript levels, the strong correlation of relative levels between samples, as well as the link with lens-specific function can be explained by a transfer of the lens material during isolation of the retina, as was reported by Kamphuis et al.<sup>78</sup> Previously, Rumyantseva et al.<sup>79</sup> found extreme downregulation of mRNA of  $\alpha$ -crystallins in OXYS lens during cataract formation. This could partly account for the observed variability. However, the functions of crystallins extend far beyond lens. In the mouse retina, crystallins were found among the most abundantly expressed transcripts.<sup>24</sup> Crystallins serve as cell protectors and function as chaperones by preventing aggregation and misfolding of proteins. Furthermore, their ability to prevent apoptosis by inhibiting caspases implies that crystallins serve crucial physiological functions.<sup>80</sup> Changes in crystallin gene expression have been reported in different models of retinal degeneration.<sup>23,77,78</sup> Elevated levels of some crystallin transcripts were observed in animal models of diabetic retina and experimental uveitis. It is known that the chaperone activity of crystallins is reduced with aging. This decrease in function may result in progressive accumulation of misfolded proteins and, thus, make the retina unable to cope with various stresses, such as hypoxia, oxidative stress and injury.<sup>81</sup> Studies on gene knockouts of  $\alpha$ -crystallins revealed that the lack of  $\alpha$ -crystallins renders RPE cells more susceptible to apoptosis from oxidative stress.<sup>82</sup> The effect of hypoxia on expression of crystallins varies in different cell types and types of hypoxia: after chemical hypoxia,  $\alpha$ B-crystallin showed an initial increase in expression followed by downregulation at later time points.<sup>83</sup> Therefore, chronic hypoxia may provoke a deficit of crystallins. As described by Markovets et al.<sup>32</sup> OXYS rats exhibit rapid expansion of the number of choriocapillaris with stasis and thrombosis during retinopathy progression. This leads to complete atrophy of choriocapillaris, which points to ischemic conditions in underlying retina layers. Moreover,  $\alpha$ B-crystallin controls folding and secretion of Vegf-A, and  $\alpha$ B-knockout mice have a lowered Vegf-A level.<sup>84</sup> Interestingly, clinical signs of retinopathy in OXYS rats manifest themselves by age 3 mo against the background of reduced Vegf-A expression.<sup>32</sup> Our data indicate that transcriptional downregulation of crystallins in OXYS retina may represent a lack of adequate stress response required for protection of

retinal neurons from damage by environmental and metabolic stress.

In addition to wound-response genes, the list of DEGs at 18 mo with aggravated stage of retinopathy is enriched by oxidation reduction players that consist mostly of oxidative stress-related genes (e.g., Nqo1, Xdh, Cdo1 and Cbr1). Among them, we found decreased expression of antioxidant enzymes catalyzing the reaction with reduced glutathione (Gpx2 and Gstm4) and oxidoreductases of the thioredoxin family of proteins (Glr1 and Txn1) that regulate the thiol redox state and protect cells and tissues from oxidative stress.<sup>85</sup> The decreased levels of thioredoxins in OXYS rats can be linked to the increased oxidative damage of proteins and lipids previously identified in this strain,<sup>86,87</sup> confirming the high sensitivity of OXYS rats to endogenous oxidative stress. Oxidative stress is an important factor for AMD progression.<sup>88</sup> Data obtained by Synowiec et al.<sup>89</sup> suggest a possible role of the genetic polymorphisms in enzymes participating in the generation and removal of iron-mediated oxidation in the AMD pathogenesis. The mRNA levels of GSTM1 and GSTM5 were significantly reduced in AMD vs. age-matched controls in human retina.<sup>90</sup> Increased oxidative stress and the accumulation of oxidatively damaged molecules lead to the dysfunction of various metabolic and signaling pathways, which, in turn, causes retinal cell death or malfunction.<sup>50</sup> The results thus reveal the involvement of oxidative stress in the progression of retinopathy in OXYS rats.

Maintenance of thiol homeostasis is important for normal mitochondrial function, and dysregulation of protein thiol homeostasis by oxidative stress leads to mitochondrial dysfunction and neurodegeneration.<sup>91</sup> For example, Grx1 is essential for maintenance of mitochondrial complex I activity, and downregulation of Grx1 results in a loss of complex I activity<sup>92</sup> through oxidation of critical thiol groups in complex I subunits. Increasing evidence shows that mitochondrial dysfunction plays a role in development and progression of AMD.<sup>93</sup> Mitochondrial dysfunctions building up with age are thought to be a causal factor for accelerated senescence in OXYS rats.<sup>30,94,95</sup> The results of the present study support this proposition. We observed significant differences in the transcriptional level of mitochondrial genes in OXYS rats compared with the Wistar strain (Table S3). Significantly decreased expression was found for Cox8b (cytochrome c oxidase, subunit VIIIb), an enzyme of the mitochondrial respiratory chain that also participates in drug resistance and the Alzheimer disease pathway.<sup>96</sup> It is noteworthy that at the age of 3 mo, the mRNA levels of many mitochondrial genes in the OXYS retina were the same as those of 18-mo-old Wistar rats. A deficiency in mitochondrial function may underlie the abnormal oxidative and tissue stress responses observed in OXYS rats.

Regulation of apoptosis is essential for maintaining functional RPE, photoreceptors and inner nuclear layer cells.<sup>97</sup> Enhanced apoptosis in RPE under inflammatory stimuli and oxidative stress was evident in murine model of AMD.<sup>98</sup> Histological examination of OXYS retinas revealed significant abnormalities of photoreceptors associated and ganglia neurons and a significant reduction of specific area of RPE, which could possibly be a result of apoptosis.<sup>28,32</sup> Not surprisingly, in the present study,

several components of signaling pathways known to inhibit apoptosis (Birc3, Cdc2, Bcl2l10, Aven and others) demonstrated downregulated expression in 3-mo-old OXYS rats. Most interestingly, Hmgb1, which is considered a marker of late apoptosis,<sup>99</sup> was found greatly upregulated in the OXYS retina at both ages (Fold change = 13.0, DESeq). Nonetheless, expression of Cflar, which encodes a protein capable of preventing apoptosis and programmed necrosis by inhibiting caspase-8,<sup>100</sup> was upregulated at age 3 mo, which may serve a compensatory function.

We also found gene expression changes for retinoid-processing proteins at 18 mo of age (Crabp1, Crabp2, Adh2, Retsat, Cyp3a9 and others) which have been previously shown to be associated with AMD.<sup>101</sup> For example, Crabp1 regulates retinoid biosynthesis by direct binding to retinoic acid, which controls RPE differentiation, proliferation, melanogenesis, angiogenesis gene expression and expression of the visual cycle genes.<sup>101</sup> Retsat converts all-trans-retinol (vitamin A) to all-trans-13,14-dihydroretinol and can participate in stress resistance.<sup>102</sup> These findings suggest that the late stage of AMD-like retinopathy in OXYS rats is accompanied by disruption of key retinoid-related functions.

We have uncovered among DEGs a cluster of genes sensitive to changes in calcium levels (Calm 4, Rcn1, Calml3, Camk1g, Tacstd2, Clca2 and others) including intermediate messenger proteins that transduce calcium signals by binding a calcium ion and then modifying its interactions with various target proteins.<sup>103</sup> In addition, we found more than 2-fold downregulation of annexin family proteins (Anxa1, Anxa2, Anxa8 and Anxa9) at both ages. Annexins belong to the family of Ca<sup>2+</sup>-dependent phospholipid binding proteins, which bind to cellular membranes in a calcium-dependent manner. Although they were originally described as a phospholipase A2-inhibitors, they also suppress various other components of the inflammatory response, such as firm adhesion of leukocytes to endothelium.<sup>104,105</sup> However, expression of phospholipases A2 (Pla2g7 and Pla2g2c) is also significantly decreased in OXYS rats.

Another group of Ca<sup>2+</sup>-binding proteins downregulated in the OXYS retina is S100 family proteins (e.g., S100a4, S100a11, S100a6 and S100a9). S100 proteins have been implicated in a variety of intracellular and extracellular functions: regulation of enzyme activities, the dynamics of cytoskeleton constituents, cell growth and differentiation and Ca<sup>2+</sup> homeostasis.<sup>106</sup> Recently Bao et al.<sup>107</sup> showed that S100A6 regulates endothelial cell cycle progression. Its depletion elevated  $\beta$ -galactosidase expression, which is a hallmark of cellular senescence. The observed dysregulated expression of Ca<sup>2+</sup>-binding proteins in OXYS retinas could be a downstream effect of altered Wnt signaling pathway (Wnt7b, Wnt10a, Wnt4 and Sfrp4). WNT-Ca<sup>2+</sup> signaling is mediated by G-proteins and phospholipases and leads to transient increases in cytoplasmic free calcium. Possible causes of dysregulated expression of Ca<sup>2+</sup>-binding proteins in OXYS rats, such as possible impairment in calcium homeostasis due to the changes in WNT-Ca<sup>2+</sup> signaling, await further investigation.

We found remarkable concerted downregulation of serine proteases (Tmprss11b, Tmprss11d, Tmprss11f, Tmprss4, Tmprss11g, Prss22, Prss27, Prss32, Klk9 and Klk13) in the 3-mo-old OXYS retina. Several studies have pointed out the role of serine

proteases in the CNS. During neural development, serine proteases contribute to cell migration, axon outgrowth and synapse elimination. In adult animals, they play a role in neuropeptide processing, regulation of neuronal survival and structural plasticity associated with learning and memory processes.<sup>108</sup> Their mechanism of action probably involves degradation of extracellular matrix components. Impaired proteolysis is associated with a broad range of neurological diseases,<sup>109</sup> but to our knowledge it has never been mentioned in the context of AMD research.

Maybe compensatory, direct inhibitors of serine protease activity were also significantly underexpressed in OXYS samples: Serpinb5, Serpinb8, Serpinb3a, Serpinb11 and Serpinb1a. The function of most members of the serpin family is to regulate the breakdown of proteins by inhibiting the catalytic activity of proteinases. Through this mechanism of action, serpins regulate a number of cellular processes, including phagocytosis, coagulation and fibrinolysis.<sup>108</sup> Also they are involved in cell adhesion and play a role in extracellular matrix remodeling.<sup>109</sup>

Significant differences were also observed in the expression of genes regulating cell adhesion. On the one hand, the expression level of some integral membrane genes mediating cell-cell and cell-matrix interactions (Cldn7, Cldn23, Cldn4 and Sdc1) was decreased. On the other hand, cadherins from the family of calcium-dependent cell-cell adhesion molecules (Pcdhgb6, Pcdhga9, Cdh19 and Pcdh21) were overexpressed in 3-mo-old OXYS retinas. Abnormal interactions between retinal layers may cause retinal detachment. Striking downregulation of 12 genes from the intermediate filament (IFs) protein family, consisting of cytoskeletal components, e.g., Krt2, Krt14 and Krt12, was observed in the interstrain comparison of 3-mo-old rats. IFs appear to play a general role in maintaining the structural integrity of Muller-cell endfeet and the inner retinal layers under mechanical stress. Furthermore, the absence of IFs in Muller cells leads to an abnormal response of the vascular system to ischemia.<sup>110,111</sup> It is possible that downregulation of IFs can lead to improper cell-cell and cell-matrix interactions. Recently Yuan et al.<sup>112</sup> analyzed the proteome of early/middle-stage AMD, and the results were indicative of hematologic malfunctions, weakened ECM structural integrity and disrupted ECM cellular interactions. Given that OXYS rats exhibit significant changes in the content and composition of extracellular proteoglycans in the brain,<sup>113</sup> alterations of expression of genes regulating cell adhesion can be related to the systemic neurodegeneration observed in OXYS rats.<sup>114</sup>

Summing up, our results indicate that combining different methods for reads counting is required for adequate detection of DE genes. Among DEGs, we uncovered several pathways involved in OXYS AMD-like retinopathy: immune response (including inflammation), apoptosis, Ca<sup>2+</sup> homeostasis and oxidative stress. Aging had significant effects on the expression of inflammatory genes, but their composition was different in the retina of OXYS and Wistar rats. Individual differences observed with aging occur not only in rodents, but also in humans. Currently there is an active search for effective molecular targets for AMD diagnostics and therapeutics and for ways to suppress the immune responsiveness. Promising treatments include anti-inflammatory

drugs based on corticosteroid and complement inhibitors.<sup>115</sup> But our investigation of OXYS rats showed that retinopathy similar to AMD in its clinical and morphological manifestations can be accompanied by downregulation of immune response genes in the retina. This indicates that any disturbances in immune defenses can accompany retinal disease, not only upregulation, but also downregulation, which can be explained within the framework of immunosenescence theory. Why some individuals develop AMD with age, whereas others do not, and why different individuals develop different AMD phenotypes are probably due to their different lifestyles and environmental risk factors. Our data support the view that the genetic background has a profound impact on AMD development and on AMD-like retinopathy in OXYS rats. With an improved understanding of the underlying genetic susceptibility, we can hope to identify therapeutic targets to halt early disease and to prevent its progression and vision loss.<sup>116</sup>

## Materials and Methods

All animal procedures were in compliance with the Association for Research in Vision and Ophthalmology statement for the Use of Animals in Ophthalmic and Vision Research and the European Communities Council Directive 86/609/ EES. All manipulations with rats were approved by Institutional Review Board 9 of the Institute of Cytology and Genetics, Siberian Branch of the Russian Academy of Sciences, according to The Guidelines for Manipulations with Experimental Animals. Male senescence-accelerated OXYS (n = 6) and age-matched male Wistar (n = 6) rats (as controls) at the age of 3 and 18 mo were obtained from the Shared Center for Genetic Resources of the Institute of Cytology and Genetics, Siberian Branch of the Russian Academy of Sciences.

**Ophthalmoscopic examination.** Ophthalmoscopic examination of all animals was performed using a Beta direct ophthalmoscope equipped with a slit lamp after dilatation with 1% tropicamide. Assessment of stages of retinopathy was performed according to “age-related eye disease study” (AREDS) grade protocol (<http://eyephoto.opth.wisc.edu>). The status of 3-mo-old OXYS rats’ fundus of eye corresponded to the first stage of the AMD: drusen with signs of atrophy of RPE and a partial loss of choriocapillaris, whereas the major blood vessels of the choroid remained unchanged. At the age of 18 mo OXYS rats had features of the second stage AMD: large soft drusen, edema in the central zone, enlargement of the zone, exudative detachment of pigmented and neuroepithelium of the retina. In comparison, none of the retinal lesions were found in Wistar rats.<sup>12,18</sup>

**RNA isolation.** Rats were euthanized using CO<sub>2</sub> inhalation. The chorioretinal complex was excised rapidly, placed in RNAlater (Ambion, Cat. #AM7020), frozen and stored at -20°C prior to analysis. Frozen rat tissues were lysed in TRIzol Reagent, and total RNA was isolated according to the manufacturer’s protocol (Invitrogen, Cat. #15596-018). RNA quality and quantity were assessed using Agilent Bioanalyser (Agilent).

**Illumina sequencing.** The RNA samples were sequenced using an Illumina Genome Analyzer IIX platform at “Genoanalitika”

Lab) in accordance with Illumina protocols for sequencing mRNA samples (mRNA-Seq Sample Prep Kit, Cat. #1004816). Briefly, poly-A tailed mRNA was purified from total RNA using Sera-Mag Magnetic Oligo (dT) beads and then fragmented into small pieces using divalent cations and heating. Using reverse transcriptase and random primers, the cleaved RNA fragments were then used to synthesize the first and second strand cDNAs. The cDNA was processed in an end repair reaction with T4 DNA polymerase and Klenow DNA polymerase in order to blunt termini. An “A” base was then added to the 3' end of the blunt phosphorylated DNA fragments, and an Illumina adaptor with a single “T” base overhang at its 3' end was then ligated to the end of the DNA fragment, for hybridization in a single-read flow cell. After the ligation reaction, a size range of cDNA templates was selected, and these fragments were amplified on a cluster station using Single-Read Cluster Generation Kit v2. Sequencing-by-synthesis (SBS) of 50-nucleotide length was performed on a Genome Analyzer IIx running SCS2.8 software using SBS v4 reagents (Illumina, Cat. #FC-940-4001). Each RNA sample was sequenced in one lane, generating over 10 million reads of 50 bases long in each sample. Images taken during the sequencing reactions were analyzed using Illumina software pipelines.

**Mapping.** Approximately 10 million single-end reads of 50-bp length were obtained for each of the 12 samples using Illumina non-stranded sequencing. After barcode trimming, the sequencing data were assessed for quality using the FastQC software and mapped to the *Rattus norvegicus* reference genome assembly RGSC 3.4 (Ensemble release 69) using TopHat v2.0.4 splice-junction mapper in “b2-sensitive” mode.<sup>117</sup> Reads mapped to gene regions were counted using the HTseq-count utility.

**Gene expression analysis.** The resulting gene count table was analyzed for differentially expressed genes (DEG) using the DESeq R package based on negative binomial distribution modeling, applying general linear models (GLM) functionality to a two-conditional design. Genes with counts in the lowest 40% quintile were filtered out prior to statistical testing. DESeq generates a log<sub>2</sub>-fold change for each gene, and Benjamini-Hochberg adjusted p values are calculated to statistically test the measured DE. Genes that failed to converge to GLM in DEG analysis were excluded. The filtered data set was subjected to variance-stabilizing transformation (vst) in order to appropriately cluster and visualize the data. Alternatively, TopHat mappings were

subjected to pairwise DEG analysis using the Cufflinks software tools with default parameters. Differential transcript expression was then computed using Cuffdiff.

**qRT-PCR.** Two micrograms of RNA were converted to cDNA using M-Mulv reverse transcriptase and random primers (Sintol, Cat. #PMM-01). The nucleotide sequences were retrieved from the GenBank database (National Center for Biotechnology Information). For PCR primer design for selected sequences Primer-BLAST was used. Primer pairs were separated by at least one intron on the corresponding genomic DNA. The primers were synthesized by Biosynthesis as shown in Table S1. For PCR analysis, the samples were amplified in duplicate using SYBR Green, Hot-Start Taq polymerase (Sibenzyme, Cat. #E351) with 200 nM of gene-specific primers and run on the CFX amplifier (Bio-Rad) using the following program: a 3 min pre-heating at 95°C, followed by 40 cycles of the following: 20 sec at 95°C, 20 sec at 60°C and 20 sec at 72°C. The data were normalized relative to the expression level of the Rpl30 gene. Unique amplification products and absence of primer-dimers was assessed using melt curve analysis and electrophoresis.

**Pathway analysis.** A bioinformatics approach was used to determine the biological context of the large amounts of gene expression RNA-Seq data. Gene lists from comparisons showing significant differences in gene expression were submitted to the free Database for Annotation, Visualization and Integrated Discovery (DAVID).<sup>48</sup> Also functional annotation was done using the WEB-based GEne SeT AnaLysis Toolkit (WebGestalt: <http://bioinfo.vanderbilt.edu/webgestalt/option.php>). All rat genes set as background.

#### Disclosure of Potential Conflicts of Interest

No potential conflicts of interest were disclosed.

#### Acknowledgments

This work has been supported by Russian Foundation for Basic Research (project 11-04-00666-a, 12-04-00091-a and 12-04-31975) and Presidium of RAS “Fundamental Sciences for Medicine.”

#### Supplemental Materials

Supplemental materials may be found here: [www.landesbioscience.com/journals/cc/article/24825](http://www.landesbioscience.com/journals/cc/article/24825)

#### References

- Newman AM, Gallo NB, Hancox LS, Miller NJ, Radeke CM, Maloney MA, et al. Systems-level analysis of age-related macular degeneration reveals global biomarkers and phenotype-specific functional networks. *Genome Med* 2012; 4:16; PMID:22364233; <http://dx.doi.org/10.1186/gm315>
- Liu MM, Chan CC, Tuo J. Genetic mechanisms and age-related macular degeneration: common variants, rare variants, copy number variations, epigenetics, and mitochondrial genetics. *Hum Genomics* 2012; 6:13; PMID:23244519; <http://dx.doi.org/10.1186/1479-7364-6-13>
- Blagosklonny MV. Prospective treatment of age-related diseases by slowing down aging. *Am J Pathol* 2012; 181:1142-6; PMID:22841821; <http://dx.doi.org/10.1016/j.ajpath.2012.06.024>
- Blagosklonny MV. Validation of anti-aging drugs by treating age-related diseases. *Aging (Albany NY)* 2009; 1:281-8; PMID:20157517
- Zhao C, Vollrath D. mTOR pathway activation in age-related retinal disease. *Aging (Albany NY)* 2011; 3:346-7; PMID:21483039
- Demidenko ZN, Blagosklonny MV. The purpose of the HIF-1/PHD feedback loop: to limit mTOR-induced HIF-1 $\alpha$ . *Cell Cycle* 2011; 10:1557-62; PMID:21521942; <http://dx.doi.org/10.4161/cc.10.10.15789>
- Gems D, Partridge L. Genetics of longevity in model organisms: debates and paradigm shifts. *Annu Rev Physiol* 2013; 75:621-44; PMID:23190075; <http://dx.doi.org/10.1146/annurev-physiol-030212-183712>
- Stipp D. A new path to longevity. *Sci Am* 2012; 306:32-9; PMID:22279832; <http://dx.doi.org/10.1038/scientificamerican0112-32>
- Blagosklonny MV. Answering the ultimate question “what is the proximal cause of aging?”. *Aging (Albany NY)* 2012; 4:861-77; PMID:23425777
- Gems D, Guardia YD. Alternative Perspectives on Aging in *Caenorhabditis elegans*: Reactive Oxygen Species or Hyperfunction? *Antioxid Redox Signal* 2012; PMID:22870907; <http://dx.doi.org/10.1089/ars.2012.4840>
- Dreesen O, Stewart CL. Accelerated aging syndromes, are they relevant to normal human aging? *Aging (Albany NY)* 2011; 3:889-95; PMID:21931180
- Tacutu R, Budovsky A, Yanai H, Fraifeld VE. Molecular links between cellular senescence, longevity and age-related diseases - a systems biology perspective. *Aging (Albany NY)* 2011; 3:1178-91; PMID:22184282
- Blagosklonny MV. Once again on rapamycin-induced insulin resistance and longevity: despite of or owing to. *Aging (Albany NY)* 2012; 4:350-8; PMID:22683661

14. Blagosklonny MV. Cell cycle arrest is not yet senescence, which is not just cell cycle arrest: terminology for TOR-driven aging. *Aging (Albany NY)* 2012; 4:159-65; PMID:22394614
15. Pani G. From growing to secreting: new roles for mTOR in aging cells. *Cell Cycle* 2011; 10:2450-3; PMID:21720215; <http://dx.doi.org/10.4161/cc.10.15.16886>
16. Blagosklonny MV. Hormesis does not make sense except in the light of TOR-driven aging. *Aging (Albany NY)* 2011; 3:1051-62; PMID:22166724
17. Lutz CT, Quinn LS. Sarcopenia, obesity, and natural killer cell immune senescence in aging: altered cytokine levels as a common mechanism. *Aging (Albany NY)* 2012; 4:535-46; PMID:22935594
18. Stefanatos R, Sanz A. Mitochondrial complex I: a central regulator of the aging process. *Cell Cycle* 2011; 10:1528-32; PMID:21471732; <http://dx.doi.org/10.4161/cc.10.10.15496>
19. Zahn JM, Poosala S, Owen AB, Ingram DK, Lustig A, Carter A, et al. AGEMAP: a gene expression database for aging in mice. *PLoS Genet* 2007; 3:e201; PMID:18081424; <http://dx.doi.org/10.1371/journal.pgen.0030201>
20. Wood SH, Craig T, Li Y, Merry B, De Magalhães JP. Whole transcriptome sequencing of the aging rat brain reveals dynamic RNA changes in the dark matter of the genome. *Age (Dord)*
21. Gamsiz ED, Ouyang Q, Schmidt M, Nagpal S, Morrow EM. Genome-wide transcriptome analysis in murine neural retina using high-throughput RNA sequencing. *Genomics* 2012; 99:44-51; PMID:22032952; <http://dx.doi.org/10.1016/j.ygeno.2011.09.003>
22. Brooks MJ, Rajasimha HK, Roger JE, Swaroop A. Next-generation sequencing facilitates quantitative analysis of wild-type and Nrl(-/-) retinal transcriptomes. *Mol Vis* 2011; 17:3034-54; PMID:22162623
23. Kandpal RP, Rajasimha HK, Brooks MJ, Nellissery J, Wan J, Qian J, et al. Transcriptome analysis using next generation sequencing reveals molecular signatures of diabetic retinopathy and efficacy of candidate drugs. *Mol Vis* 2012; 18:1123-46; PMID:22605924
24. Mustafa D, Maeda T, Kohno H, Nadeau JH, Palczewski K. Inflammatory priming predisposes mice to age-related retinal degeneration. *J Clin Invest* 2012; 122:2989-3001; PMID:22797304; <http://dx.doi.org/10.1172/JCI64427>
25. Mustafa D, Kevany BM, Genoud C, Okano K, Cideciyan AV, Sumaroka A, et al. Defective photoreceptor phagocytosis in a mouse model of enhanced S-cone syndrome causes progressive retinal degeneration. *FASEB J* 2011; 25:3157-76; PMID:21659555; <http://dx.doi.org/10.1096/fj.11-186767>
26. Nagalakshmi U, Wang Z, Waern K, Shou C, Raha D, Gerstein M, et al. The transcriptional landscape of the yeast genome defined by RNA sequencing. *Science* 2008; 320:1344-9; PMID:18451266; <http://dx.doi.org/10.1126/science.1158441>
27. Kolosova NG, Muraleva NA, Zhdankina AA, Stefanova NA, Fursova AZ, Blagosklonny MV. Prevention of age-related macular degeneration-like retinopathy by rapamycin in rats. *Am J Pathol* 2012; 181:472-7; PMID:22683466; <http://dx.doi.org/10.1016/j.ajpath.2012.04.018>
28. Zhdankina AA, Fursova AZH, Logvinov SV, Kolosova NG. Clinical and morphological characteristics of chorioretinal degeneration in early aging OXYS rats. *Bull Exp Biol Med* 2008; 146:455-8; PMID:19489319; <http://dx.doi.org/10.1007/s10517-009-0298-4>
29. Neroev VV, Archipova MM, Bakeeva LE, Fursova AZH, Grigorian EN, Grishanova AY, et al. Mitochondria-targeted plastoquinone derivatives as tools to interrupt execution of the aging program. 4. Age-related eye disease. SkQ1 returns vision to blind animals. *Biochemistry (Mosc)* 2008; 73:1317-28; PMID:19120017; <http://dx.doi.org/10.1134/S0006297908120043>
30. Saprunova VB, Lelekova MA, Kolosova NG, Bakeeva LE. SkQ1 slows development of age-dependent destructive processes in retina and vascular layer of eyes of wistar and OXYS rats. *Biochemistry (Mosc)* 2012; 77:648-58; PMID:22817465; <http://dx.doi.org/10.1134/S0006297912060120>
31. Saprunova VB, Pilipenko DI, Alexeevsky AV, Fursova AZH, Kolosova NG, Bakeeva LE. Lipofuscin granule dynamics during development of age-related macular degeneration. *Biochemistry (Mosc)* 2010; 75:130-8; PMID:20367599; <http://dx.doi.org/10.1134/S0006297910020021>
32. Markovets AM, Saprunova VB, Zhdankina AA, Fursova AZH, Bakeeva LE, Kolosova NG. Alterations of retinal pigment epithelium cause AMD-like retinopathy in senescence-accelerated OXYS rats. *Aging (Albany NY)* 2011; 3:44-54; PMID:21191149
33. Markovets AM, Fursova AZ, Kolosova NG. Therapeutic action of the mitochondria-targeted antioxidant SkQ1 on retinopathy in OXYS rats linked with improvement of VEGF and PEDF gene expression. *PLoS ONE* 2011; 6:e21682; PMID:21750722; <http://dx.doi.org/10.1371/journal.pone.0021682>
34. Zheng XF. Chemoprevention of age-related macular regeneration (AMD) with rapamycin. *Aging (Albany NY)* 2012; 4:375-6; PMID:22796653
35. Korbolina EE, Kozhevnikova OS, Stefanova NA, Kolosova NG. Quantitative trait loci on chromosome 1 for cataract and AMD-like retinopathy in senescence-accelerated OXYS rats. *Aging (Albany NY)* 2012; 4:49-59; PMID:22300709
36. Trapnell C, Williams BA, Pertea G, Mortazavi A, Kwan G, van Baren MJ, et al. Transcript assembly and quantification by RNA-Seq reveals unannotated transcripts and isoform switching during cell differentiation. *Nat Biotechnol* 2010; 28:511-5; PMID:20436464; <http://dx.doi.org/10.1038/nbt.1621>
37. Robles JA, Qureshi SE, Stephen SJ, Wilson SR, Burden CJ, Taylor JM. Efficient experimental design and analysis strategies for the detection of differential expression using RNA-Sequencing. *BMC Genomics* 2012; 13:484; PMID:22985019; <http://dx.doi.org/10.1186/1471-2164-13-484>
38. Anders S, Huber W. Differential expression analysis for sequence count data. *Genome Biol* 2010; 11:R106; PMID:20979621; <http://dx.doi.org/10.1186/gb-2010-11-10-r106>
39. Bonilla IE, Tanabe K, Strittmatter SM. Small proline-rich repeat protein 1A is expressed by axotomized neurons and promotes axonal outgrowth. *J Neurosci* 2002; 22:1303-15; PMID:11850458
40. Starkey ML, Davies M, Yip PK, Carter LM, Wong DJ, McMahon SB, et al. Expression of the regeneration-associated protein SPRR1A in primary sensory neurons and spinal cord of the adult mouse following peripheral and central injury. *J Comp Neurol* 2009; 513:51-68; PMID:19107756; <http://dx.doi.org/10.1002/cne.21944>
41. Swamynathan S, Buela KA, Kington P, Lathrop KL, Misawa H, Hendricks RL, et al. Klf4 regulates the expression of Slurp1, which functions as an immunomodulatory peptide in the mouse cornea. *Invest Ophthalmol Vis Sci* 2012; 53:8433-46; PMID:23139280; <http://dx.doi.org/10.1167/iovs.12-10759>
42. Chimenti F, Hogg RC, Plantard L, Lehmann C, Brackh N, Fischer J, et al. Identification of SLURP-1 as an epidermal neuromodulator explains the clinical phenotype of Mal de Meleda. *Hum Mol Genet* 2003; 12:3017-24; PMID:14506129; <http://dx.doi.org/10.1093/hmg/ddg320>
43. Bianco AC, Salvatore D, Gereben B, Berry MJ, Larsen PR. Biochemistry, cellular and molecular biology, and physiological roles of the iodothyronine selenoenzymes. *Endocr Rev* 2002; 23:38-89; PMID:11844744; <http://dx.doi.org/10.1210/er.23.1.38>
44. Dennis G Jr., Sherman BT, Hosack DA, Yang J, Gao W, Lane HC, et al. DAVID: Database for Annotation, Visualization, and Integrated Discovery. *Genome Biol* 2003; 4:3; PMID:12734009; <http://dx.doi.org/10.1186/gb-2003-4-5-p3>
45. Lisanti MP, Martinez-Outschoorn UE, Lin Z, Pavlides S, Whitaker-Menezes D, Pestell RG, et al. Hydrogen peroxide fuels aging, inflammation, cancer metabolism and metastasis: the seed and soil also needs "fertilizer". *Cell Cycle* 2011; 10:2440-9; PMID:21734470; <http://dx.doi.org/10.4161/cc.10.15.16870>
46. Kaarniranta K, Kauppinen A. Inflammaging: disturbed interplay between autophagy and inflammasomes. *Salminen A. Aging (Albany, NY Online)* 2012; 4:166-75
47. Cai D, Liu T. Inflammatory cause of metabolic syndrome via brain stress and NF-κB. *Aging (Albany, NY Online)* 2012; 4:98-115
48. Chen H, Liu B, Lukas TJ, Neufeld AH. The aged retinal pigment epithelium/choroid: a potential substratum for the pathogenesis of age-related macular degeneration. *PLoS ONE* 2008; 3:e2339; PMID:18523633; <http://dx.doi.org/10.1371/journal.pone.0002339>
49. Chen M, Muckersiege E, Forrester JV, Xu H. Immune activation in retinal aging: a gene expression study. *Invest Ophthalmol Vis Sci* 2010; 51:5888-96; PMID:20538981; <http://dx.doi.org/10.1167/iovs.09-5103>
50. Xu H, Chen M, Forrester JV. Para-inflammation in the aging retina. *Prog Retin Eye Res* 2009; 28:348-68; PMID:19560552; <http://dx.doi.org/10.1016/j.preteyeres.2009.06.001>
51. Landis G, Shen J, Tower J. Gene expression changes in response to aging compared to heat stress, oxidative stress and ionizing radiation in *Drosophila melanogaster*. *Aging (Albany NY)* 2012; 4:768-89; PMID:23211361
52. Cai H, Fields MA, Hoshino R, Priore LV. Effects of aging and anatomic location on gene expression in human retina. *Front Aging Neurosci* 2012; 4:8; PMID:22666212; <http://dx.doi.org/10.3389/fnagi.2012.00008>
53. Anand PK, Malireddi RKS, Lukens JR, Vogel P, Bertin J, Lamkanfi M, et al. NLRP6 negatively regulates innate immunity and host defence against bacterial pathogens. *Nature* 2012; 488:389-93; PMID:22763455; <http://dx.doi.org/10.1038/nature11250>
54. Patel M, Chan CC. Immunopathological aspects of age-related macular degeneration. *Semin Immunopathol* 2008; 30:97-110; PMID:18299834; <http://dx.doi.org/10.1007/s00281-008-0112-9>
55. Forrester JV. Bowman lecture on the role of inflammation in degenerative disease of the eye. *Eye (Lond)* 2013; 27:340-52; PMID:23288138; <http://dx.doi.org/10.1038/eye.2012.265>
56. Hageman GS, Anderson DH, Johnson LV, Hancox LS, Taiber AJ, Hardisty LI, et al. A common haplotype in the complement regulatory gene factor H (HF1/CFH) predisposes individuals to age-related macular degeneration. *Proc Natl Acad Sci USA* 2005; 102:7227-32; PMID:15870199; <http://dx.doi.org/10.1073/pnas.0501536102>
57. Tuo J, Grob S, Zhang K, Chan CC. Genetics of immunological and inflammatory components in age-related macular degeneration. *Ocul Immunol Inflamm* 2012; 20:27-36; PMID:22324898; <http://dx.doi.org/10.3109/09273948.2011.628432>
58. Zarepari S, Branham KEH, Li M, Shah S, Klein RJ, Ott J, et al. Strong association of the Y402H variant in complement factor H at 1q32 with susceptibility to age-related macular degeneration. *Am J Hum Genet* 2005; 77:149-53; PMID:15895326; <http://dx.doi.org/10.1086/431426>
59. Akiyama H, Barger S, Barnum S, Bradt B, Bauer J, Cole GM, et al. Inflammation and Alzheimer's disease. *Neurobiol Aging* 2000; 21:383-421; PMID:10858586; [http://dx.doi.org/10.1016/S0197-4580\(00\)00124-X](http://dx.doi.org/10.1016/S0197-4580(00)00124-X)

60. Mullins RF, Russell SR, Anderson DH, Hageman GS. Drusen associated with aging and age-related macular degeneration contain proteins common to extracellular deposits associated with atherosclerosis, elastosis, amyloidosis, and dense deposit disease. *FASEB J* 2000; 14:835-46; PMID:10783137
61. Anderson DH, Talaga KC, Rivest AJ, Barron E, Hageman GS, Johnson LV. Characterization of beta amyloid assemblies in drusen: the deposits associated with aging and age-related macular degeneration. *Exp Eye Res* 2004; 78:243-56; PMID:14729357; <http://dx.doi.org/10.1016/j.exer.2003.10.011>
62. Song B, Davis K, Liu XS, Lee HG, Smith M, Liu X. Inhibition of Polo-like kinase 1 reduces beta-amyloid-induced neuronal cell death in Alzheimer's disease. *Aging (Albany NY)* 2011; 3:846-51; PMID:21931181
63. Kumar S, Walter J. Phosphorylation of amyloid beta (A $\beta$ ) peptides - a trigger for formation of toxic aggregates in Alzheimer's disease. *Aging (Albany NY)* 2011; 3:803-12; PMID:21869458
64. Hageman GS, Luthert PJ, Victor Chong NH, Johnson LV, Anderson DH, Mullins RF. An integrated hypothesis that considers drusen as biomarkers of immune-mediated processes at the RPE-Bruch's membrane interface in aging and age-related macular degeneration. *Prog Retin Eye Res* 2001; 20:705-32; PMID:11587915; [http://dx.doi.org/10.1016/S1350-9462\(01\)00010-6](http://dx.doi.org/10.1016/S1350-9462(01)00010-6)
65. Damico FM, Gasparin F, Scolari MR, Pedral LS, Takahashi BS. New approaches and potential treatments for dry age-related macular degeneration. *Arq Bras Oftalmol* 2012; 75:71-6; PMID:22552424
66. Ramkumar HL, Zhang J, Chan CC. Retinal ultrastructure of murine models of dry age-related macular degeneration (AMD). *Prog Retin Eye Res* 2010; 29:169-90; PMID:20206286; <http://dx.doi.org/10.1016/j.preteyeres.2010.02.002>
67. Ambati J, Anand A, Fernandez S, Sakurai E, Lynn BC, Kuziel WA, et al. An animal model of age-related macular degeneration in senescent Ccl-2- or Ccr-2-deficient mice. *Nat Med* 2003; 9:1390-7; PMID:14566334; <http://dx.doi.org/10.1038/nm950>
68. Ding X, Patel M, Chan CC. Molecular pathology of age-related macular degeneration. *Prog Retin Eye Res* 2009; 28:1-18; PMID:19026761; <http://dx.doi.org/10.1016/j.preteyeres.2008.11.001>
69. Markova EV, Obukhova LA, Kolosova NG. Activity of cell immune response and open field behavior in Wistar and OXYS rats. *Bull Exp Biol Med* 2003; 136:377-9; PMID:14714088; <http://dx.doi.org/10.1023/B:BEBM.0000010957.87077.ae>
70. Obukhova LA, Skulachev VP, Kolosova NG. Mitochondria-targeted antioxidant SkQ1 inhibits age-dependent involution of the thymus in normal and senescence-prone rats. *Aging (Albany NY)* 2009; 1:389-401; PMID:20195490
71. Appay V, Sauce D, Prelog M. The role of the thymus in immunosenescence: lessons from the study of thymectomized individuals. *Aging (Albany NY)* 2010; 2:78-81; PMID:20354268
72. Sauce D, Appay V. Altered thymic activity in early life: how does it affect the immune system in young adults? *Curr Opin Immunol* 2011; 23:543-8; PMID:21752618; <http://dx.doi.org/10.1016/j.coi.2011.05.001>
73. Anderson DH, Radeke MJ, Gallo NB, Chapin EA, Johnson PT, Curletti CR, et al. The pivotal role of the complement system in aging and age-related macular degeneration: hypothesis re-visited. *Prog Retin Eye Res* 2010; 29:95-112; PMID:19961953; <http://dx.doi.org/10.1016/j.preteyeres.2009.11.003>
74. Elmer BM, McAllister AK. Major histocompatibility complex class I proteins in brain development and plasticity. *Trends Neurosci* 2012; 35:660-70; PMID:22939644; <http://dx.doi.org/10.1016/j.tins.2012.08.001>
75. Stevens B, Allen NJ, Vazquez LE, Howell GR, Christopherson KS, Nouri N, et al. The classical complement cascade mediates CNS synapse elimination. *Cell* 2007; 131:1164-78; PMID:18083105; <http://dx.doi.org/10.1016/j.cell.2007.10.036>
76. Yu M, Zou W, Peachey NS, McIntyre TM, Liu J. A novel role of complement in retinal degeneration. *Invest Ophthalmol Vis Sci* 2012; 53:7684-92; PMID:23074214; <http://dx.doi.org/10.1167/iovs.12-10069>
77. Xi J, Farjo R, Yoshida S, Kern TS, Swaroop A, Andley UP. A comprehensive analysis of the expression of crystallins in mouse retina. *Mol Vis* 2003; 9:410-9; PMID:12949468
78. Kamphuis W, Dijk F, Kraan W, Bergen AAB. Transfer of lens-specific transcripts to retinal RNA samples may underlie observed changes in crystallin-gene transcript levels after ischemia. *Mol Vis* 2007; 13:220-8; PMID:17327827
79. Rummyantseva YV, Fursova AZH, Fedoseeva LA, Kolosova NG. Changes in physicochemical parameters and alpha-crystallin expression in the lens during cataract development in OXYS rats. *Biochemistry (Mosc)* 2008; 73:1176-82; PMID:19120020; <http://dx.doi.org/10.1134/S0006297908110023>
80. Kamradt MC, Chen F, Cryns VL. The small heat shock protein alpha B-crystallin negatively regulates cytochrome c- and caspase-8-dependent activation of caspase-3 by inhibiting its autoproteolytic maturation. *J Biol Chem* 2001; 276:16059-63; PMID:11274139; <http://dx.doi.org/10.1074/jbc.C100107200>
81. Kerr BA, Byzova TV. alphaB-crystallin: a novel VEGF chaperone. *Blood* 2010; 115:3181-3; PMID:20413662; <http://dx.doi.org/10.1182/blood-2010-01-262766>
82. Young J, Jin M, Barron E, Spee C, Wawrousek EF, Kannan R, et al. alpha-Crystallin distribution in retinal pigment epithelium and effect of gene knockouts on sensitivity to oxidative stress. *Mol Vis* 2007; 13:566-77; PMID:17438522
83. Young J, Kannan R, Wawrousek EF, Spee C, Sreekumar PG, Hinton DR. Exacerbation of retinal degeneration in the absence of alpha crystallin in an in vivo model of chemically induced hypoxia. *Exp Eye Res* 2008; 86:355-65; PMID:18191123; <http://dx.doi.org/10.1016/j.exer.2007.11.007>
84. Kase S, He S, Sonoda S, Kitamura M, Spee C, Wawrousek E, et al. alphaB-crystallin regulation of angiogenesis by modulation of VEGF. *Blood* 2010; 115:3398-406; PMID:20023214; <http://dx.doi.org/10.1182/blood-2009-01-197095>
85. Yoshihara E, Chen Z, Matsuo Y, Masutani H, Yodoi J. Thiol redox transitions by thioredoxin and thioredoxin-binding protein-2 in cell signaling. *Methods Enzymol* 2010; 474:67-82; PMID:20609905; [http://dx.doi.org/10.1016/S0076-6879\(10\)74005-2](http://dx.doi.org/10.1016/S0076-6879(10)74005-2)
86. Sinityna O, Krysanova S, Ishchenko A, Dikalova AE, Stolyarov S, Kolosova N, et al. Age-associated changes in oxidative damage and the activity of antioxidant enzymes in rats with inherited over-generation of free radicals. *J Cell Mol Med* 2006; 10:206-15; PMID:16563232; <http://dx.doi.org/10.1111/j.1582-4934.2006.tb00301.x>
87. Kolosova NG, Shcheglova TV, Sergeeva SV, Loskutova LV. Long-term antioxidant supplementation attenuates oxidative stress markers and cognitive deficits in senescent-accelerated OXYS rats. *Neurobiol Aging* 2006; 27:1289-97; PMID:16246464; <http://dx.doi.org/10.1016/j.neurobiolaging.2005.07.022>
88. Jarrett SG, Boulton ME. Consequences of oxidative stress in age-related macular degeneration. *Mol Aspects Med* 2012; 33:399-417; PMID:22510306; <http://dx.doi.org/10.1016/j.mam.2012.03.009>
89. Synowiec E, Sliwinski T, Danisz K, Blasiak J, Sklodowska A, Romaniuk D, et al. Association between polymorphism of the NQO1, NOS3 and NFE2L2 genes and AMD. *Front Biosci* 2013; 18:80-90; PMID:23276910; <http://dx.doi.org/10.2741/4088>
90. Hunter A, Spechler PA, Cwanger A, Song Y, Zhang Z, Ying GS, et al. DNA methylation is associated with altered gene expression in AMD. *Invest Ophthalmol Vis Sci* 2012; 53:2089-105; PMID:22410570; <http://dx.doi.org/10.1167/iovs.11-8449>
91. Diwakar L, Kenchappa RS, Annepu J, Ravindranath V. Downregulation of glutaredoxin but not glutathione loss leads to mitochondrial dysfunction in female mice CNS: implications in excitotoxicity. *Neurochem Int* 2007; 51:37-46; PMID:17512091; <http://dx.doi.org/10.1016/j.neuint.2007.03.008>
92. Kenchappa RS, Ravindranath V. Glutaredoxin is essential for maintenance of brain mitochondrial complex I: studies with MPTP. *FASEB J* 2003; 17:717-9; PMID:12594173
93. Feher J, Kovacs I, Artico M, Cavallotti C, Papale A, Balacco Gabrieli C. Mitochondrial alterations of retinal pigment epithelium in age-related macular degeneration. *Neurobiol Aging* 2006; 27:983-93; PMID:15979212; <http://dx.doi.org/10.1016/j.neurobiolaging.2005.05.012>
94. Salganik RI, Shabalina IG, Solovyova NA, Kolosova NG, Solovyov VN, Kolpakov AR. Impairment of respiratory functions in mitochondria of rats with an inherited hyperproduction of free radicals. *Biochem Biophys Res Commun* 1994; 205:180-5; PMID:7999021; <http://dx.doi.org/10.1006/bbrc.1994.2647>
95. Kolosova NG, Aidagulova SV, Nepomyashchikh GI, Shabalina IG, Shalbuva NI. Dynamics of structural and functional changes in hepatocyte mitochondria of senescence-accelerated OXYS rats. *Bull Exp Biol Med* 2001; 132:814-9; PMID:11713575; <http://dx.doi.org/10.1023/A:1013014919721>
96. Maurer I, Zierz S, Möller HJ. A selective defect of cytochrome c oxidase is present in brain of Alzheimer disease patients. *Neurobiol Aging* 2000; 21:455-62; PMID:10858595; [http://dx.doi.org/10.1016/S0197-4580\(00\)0112-3](http://dx.doi.org/10.1016/S0197-4580(00)0112-3)
97. Dunaief JL, Dentechev T, Ying GS, Milam AH. The role of apoptosis in age-related macular degeneration. *Arch Ophthalmol* 2002; 120:1435-42; PMID:12427055
98. Wang Y, Shen D, Wang VM, Yu CR, Wang RX, Tuo J, et al. Enhanced apoptosis in retinal pigment epithelium under inflammatory stimuli and oxidative stress. *Apoptosis* 2012; 17:1144-55; PMID:22911474; <http://dx.doi.org/10.1007/s10495-012-0750-1>
99. Bell CW, Jiang W, Reich CF 3rd, Pisetsky DS. The extracellular release of HMGB1 during apoptotic cell death. *Am J Physiol Cell Physiol* 2006; 291:C1318-25; PMID:16855214; <http://dx.doi.org/10.1152/ajpcell.00616.2005>
100. Piao X, Komazawa-Sakon S, Nishina T, Koike M, Piao JH, Ehlken H, et al. c-FLIP maintains tissue homeostasis by preventing apoptosis and programmed necrosis. *Sci Signal* 2012; 5:ra93; PMID:23250397; <http://dx.doi.org/10.1126/scisignal.2003558>
101. Nordgaard CL, Berg KM, Kappahh RJ, Reilly C, Feng X, Olsen TW, et al. Proteomics of the retinal pigment epithelium reveals altered protein expression at progressive stages of age-related macular degeneration. *Invest Ophthalmol Vis Sci* 2006; 47:815-22; PMID:16505012; <http://dx.doi.org/10.1167/iovs.05-0976>
102. Nagaoka-Yasuda R, Matsuo N, Perkins B, Limbaeck-Stokin K, Mayford M. An RNAi-based genetic screen for oxidative stress resistance reveals retinol saturase as a mediator of stress resistance. *Free Radic Biol Med* 2007; 43:781-8; PMID:17664141; <http://dx.doi.org/10.1016/j.freeradbiomed.2007.05.008>
103. Chin D, Means AR. Calmodulin: a prototypical calcium sensor. *Trends Cell Biol* 2000; 10:322-8; PMID:10884684; [http://dx.doi.org/10.1016/S0962-8924\(00\)01800-6](http://dx.doi.org/10.1016/S0962-8924(00)01800-6)
104. Hayhoe RPG, Kamal AM, Solito E, Flower RJ, Cooper D, Perretti M. Annexin 1 and its bioactive peptide inhibit neutrophil-endothelium interactions under flow: indication of distinct receptor involvement. *Blood* 2006; 107:2123-30; PMID:16278303; <http://dx.doi.org/10.1182/blood-2005-08-3099>



105. Parente L, Solito E. Annexin 1: more than an anti-phospholipase protein. *Inflamm Res* 2004; 53:125-32; PMID:15060718; <http://dx.doi.org/10.1007/s00011-003-1235-z>
106. Donato R. Intracellular and extracellular roles of S100 proteins. *Microsc Res Tech* 2003; 60:540-51; PMID:12645002; <http://dx.doi.org/10.1002/jemt.10296>
107. Bao L, Odell AF, Stephen SL, Wheatcroft SB, Walker JH, Ponnambalam S. The S100A6 calcium-binding protein regulates endothelial cell-cycle progression and senescence. *FEBS J* 2012; 279:4576-88; PMID:23095053; <http://dx.doi.org/10.1111/febs.12044>
108. Almonte AG, Sweatt JD. Serine proteases, serine protease inhibitors, and protease-activated receptors: roles in synaptic function and behavior. *Brain Res* 2011; 1407:107-22; PMID:21782155; <http://dx.doi.org/10.1016/j.brainres.2011.06.042>
109. Molinari F, Meskanaite V, Munnich A, Sonderegger P, Colleaux L. Extracellular proteases and their inhibitors in genetic diseases of the central nervous system. *Hum Mol Genet* 2003; 12(Spec No):R195-200; PMID:12925575; <http://dx.doi.org/10.1093/hmg/ddg276>
110. Lodish H, Berk A, Zipursky SL, et al. The Dynamics of Actin Assembly. In: Freeman WH, ed. *Molecular Cell Biology*. 4th edition. NY. 2000. Section 18.2.
111. Lundkvist A, Reichenbach A, Betsholtz C, Carmeliet P, Wolburg H, Pekny M. Under stress, the absence of intermediate filaments from Müller cells in the retina has structural and functional consequences. *J Cell Sci* 2004; 117:3481-8; PMID:15226376; <http://dx.doi.org/10.1242/jcs.01221>
112. Yuan X, Gu X, Crabb JS, Yue X, Shadrach K, Hollyfield JG, et al. Quantitative proteomics: comparison of the macular Bruch membrane/choroid complex from age-related macular degeneration and normal eyes. *Mol Cell Proteomics* 2010; 9:1031-46; PMID:20177130; <http://dx.doi.org/10.1074/mcp.M900523-MCP200>
113. Rykova VI, Leberfarb EY, Stefanova NA, Shevelev OB, Dymshits GM, Kolosova NG. Brain proteoglycans in postnatal development and during behavior decline in senescence-accelerated OXYS rats. *Adv Gerontol* 2011; 24:234-43; PMID:21957580
114. Kolosova NG, Stefanova NA, Sergeeva SV. OXYS rats: a prospective model for evaluation of antioxidant availability in prevention and therapy of accelerated aging and age-related cognitive decline. In: Gariépy Q, Ménard R, eds. *Handbook of Cognitive Aging: Causes, Processes and Effects*. Nova Science Publishers, NY: 47-82.
115. Wang Y, Wang VM, Chan CC. The role of anti-inflammatory agents in age-related macular degeneration (AMD) treatment. *Eye (Lond)* 2011; 25:127-39; PMID:21183941; <http://dx.doi.org/10.1038/eye.2010.196>
116. Miller JW. Age-related macular degeneration revisited—piecing the puzzle: the LXIX Edward Jackson memorial lecture. *Am J Ophthalmol* 2013; 155:1, e13; PMID:23245386; <http://dx.doi.org/10.1016/j.ajo.2012.10.018>
117. Trapnell C, Pachter L, Salzberg SL. TopHat: discovering splice junctions with RNA-Seq. *Bioinformatics* 2009; 25:1105-11; PMID:19289445; <http://dx.doi.org/10.1093/bioinformatics/btp120>